adrenal medullary cells (7) and PC12 cells (8). These results suggest that SERMs directly affect ion channels and subsequent cellular functions in a non-genomic manner.

Adrenal medullary cells are derived from the embryonic neural crest and share many physiological and pharmacological properties with postganglionic sympathetic neurons. Stimulation of AChRs in the cells increases the synthesis of catecholamines and causes the secretion of catecholamines into the systemic circulation (9, 10). In bovine adrenal medullary cells, at least three distinct types of ionic channels are involved in catecholamine secretion (11): nAChR-ion channels, voltage-dependent Na^+ channels, and voltage-dependent Ca^{2+} channels. In these cells, previous studies have shown that either carbachol (a synthetic derivative of ACh)-induced Na^+ influx via nAChR-ion channels or veratridine-induced Na^+ influx via voltage-dependent Na^+ channels increases Ca^{2+} influx via voltage-dependent Ca^{2+} channels, a prerequisite for the secretion (7, 11) and synthesis (10) of catecholamines. In contrast, high K^+ directly gates voltage-dependent Ca^{2+} channels to increase Ca^{2+} influx without increasing Na^+ influx (11).

Previously, we reported the occurrence and pharmacological characterization of estrogen receptors in the plasma membrane of bovine adrenal medulla (12). Furthermore, phytoestrogens such as daidzein (13) and resveratrol (14) increased catecholamine synthesis through the plasma membrane estrogen receptors. In the present study, we examined the effects of two SERMs, raloxifene and tamoxifen, on [^{3}H]17β-estradiol (17β-E_2) binding to the membrane estrogen receptors, as well as catecholamine synthesis and secretion in cultured bovine adrenal medullary cells. We found that SERMs allosterically modulate [^{3}H]17β-E_2 binding to plasma membrane estrogen receptors and positively or negatively influence catecholamine synthesis and secretion in the cells.

Materials and Methods

Materials

Oxygenated Krebs-Ringer phosphate (KRP) buffer was used throughout. Its composition is as follows: 154 mM NaCl, 5.6 mM KCl, 1.1 mM $MgSO_4$, 2.2 mM $CaCl_2$, 0.85 mM NaH_2PO_4, 2.15 mM Na_2HPO_4, and 10 mM glucose, adjusted pH to 7.4. Reagents were obtained from the following sources: Eagle's minimum essential medium (MEM) (Nissui Pharmaceutical, Tokyo); calf serum (Cell Culture Technologies, Zürich, Switzerland); collagenase (Nitta Zerachin, Osaka); raloxifene, tamoxifen, 17β-E_2, ACh, veratridine (Sigma Chemical Co., St. Louis, MO, USA); [2,4,6,7-^{3}H]17β-E_2 (3515 GBq/mmol), [^{22}Na]Cl, [^{45}Ca]Cl_2, and L-[U-^{14}C]tyrosine (Perkin-Elmer, Ltd., Boston, MA, USA). Raloxifene and tamoxifen were dissolved in 100% dimethyl sulfoxide and then diluted in a reaction medium before use at a final concentration of dimethyl sulfoxide not exceeding 0.5% unless otherwise specified.

Isolation and primary culture of bovine adrenal medullary cells

Bovine adrenal medullary cells were isolated by collagenase digestion of adrenal medullary slices according to the previously reported method (15, 16). Cells were suspended in Eagle's MEM containing 10% calf serum, 3 μM cytosine arabinoside, and several antibiotics, and maintained in monolayer culture at a density of 4×10^6 cells per dish (35 mm dish; Falcon, Becton Dickinson Labware, Franklin Lakes, NJ, USA) or 10^6 cells per well (24-well plate; Corning Life Science, Lowell, MA, USA) at 37°C under a humidified atmosphere of 5% CO_2 and 95% air. The cells were used for experiments between 2 and 5 days of culture.

[^{3}H]17β-E_2 binding to plasma membranes isolated from adrenal medulla

Plasma membranes were isolated from bovine adrenal medulla as described previously (12, 13). The specific binding of [^{3}H]17β-E_2 was determined by incubating plasma membranes (30 μg protein) in Krebs-Ringer HEPES (KRH) buffer (composition: 125 mM NaCl, 4.8 mM KCl, 2.6 mM $CaCl_2$, 1.2 mM $MgSO_4$, 5.6 mM glucose, and 25 mM HEPES-Tris, pH 7.4) (final volume of 200 μL) with various concentrations (0.001 – 10 μM) of raloxifene or tamoxifen and [^{3}H]17β-E_2 (5 nM, 0.1 μCi) at 4°C for 30 min. Then [^{3}H]17β-E_2 bound to the membranes was separated from free ligand by filtration through a GF/C glass fiber filter (Whatman, Maidstone, UK), and the filter was washed 3 times with the ice-cold binding buffer. Specific binding of [^{3}H]17β-E_2 was defined as the total binding minus non-specific binding, which was determined in the presence of 17β-E_2 (1.0 μM) (12).

^{14}C-catecholamine synthesis from [^{14}C]tyrosine in the cells

After preincubation for 10 min, cells were incubated with 20 μM L-[U-^{14}C]tyrosine (1 μCi) in KRP buffer in the presence or absence of various concentrations of raloxifene or tamoxifen and 300 μM ACh at 37°C for 20 min. After removing the incubation medium by aspiration, cells were harvested in 0.4 M perchloric acid and centrifuged at 1600 × g for 10 min. ^{14}C-Labelled catechol compounds were separated further by ion exchange chromatography on Duolite C-25 columns (H^+-type, 0.4 × 7.0 cm) (10) and counted for the radioac-

tivity by a Packard Tri-Carb 2900TR liquid scintillation counter. ^{14}C-Catecholamine synthesis was expressed as the sum of the ^{14}C-catecholamines (adrenaline, noradrenaline, and dopamine).

Catecholamine secretion from cultured bovine adrenal medullary cells

The secretion of catecholamines was measured as described previously (15). After preincubation with or without raloxifene or tamoxifen at 37°C for 10 min, the cells (10^6 per well) were incubated with or without the SERMs in the presence or absence of various secretagogues at 37°C for another 10 min. After the reaction, the incubation medium was transferred immediately to a test tube containing perchloric acid (final concentration, 0.4 M). Catecholamines (noradrenaline and adrenaline) secreted into the medium were adsorbed onto aluminum hydroxide and estimated by the ethylendiamine condensation method using a fluorescence spectrophotometer (F-2500; Hitachi, Tokyo) with excitation and emission wavelengths of 420 and 540 nm, respectively.

$^{22}Na^+$ and $^{45}Ca^{2+}$ influx by the cells

The influx of $^{22}Na^+$ and $^{45}Ca^{2+}$ was measured as reported previously (11). After preincubation with or without raloxifene or tamoxifen at 37°C for 10 min, the cells (4×10^6 per dish) were incubated with 1.5 μCi of ^{22}NaCl or 1.5 μCi of $^{45}CaCl_2$ at 37°C for 5 min in the presence or absence of 300 μM ACh and various concentrations of the SERMs in KRP buffer. After incubation, the cells were washed 3 times with ice-cold KRP buffer, solubilized in 10% Triton X-100, and counted for radioactivity of $^{22}Na^+$ and $^{45}Ca^{2+}$ by an Aloka ARC-2005 gamma counter and a Packard Tri-Carb 2900TR liquid scintillation counter, respectively.

Expression of nAChRs in Xenopus oocytes and electrophysiological recordings

Isolation and microinjection of *Xenopus* oocytes was performed as described previously (17, 18). In brief, the cDNA encoding the $\alpha 4$ and $\beta 2$ subunits of rat neuronal nAChR, subcloned into pcDNAI/Neo (Invitogen, Carlsbad, CA, USA) vector, was kindly provided from Dr. James W. Patrick (Division of Neuroscience, Baylor College of Medicine, Houston, TX, USA). Oocytes were injected with cDNAs (1.5 ng/30 nL) and electrophysiological recordings were performed 2 – 3 days after injection. Each oocyte was perfused (2 mL/min) with Ba^{2+}-Ringer's solution (115 mM NaCl, 2.5 mM KCl, 1.8 mM $BaCl_2$, and 10 mM HEPES, pH 7.4) containing 1 μM atropine sulfate, to minimize the effects of secondary activated Ca^{2+}-dependant Cl^- currents and then impaled with 2 glass electrodes (1 – 5 MΩ) filled with 3 M KCl and clamped at −70 mV using the OC-725C Oocyte Clamp Amplifier (Harvard Apparatus, Inc., Holliston, MA, USA). ACh was applied for 30 s to obtain the maximum (peak) current used as a measure of drug response. We examined the effect of raloxifene (1 μM) on Na^+ current induced by ACh at a concentration that produced 50% of the maximal effect (EC_{50}) of ACh (1 mM).

Statistical analyses

All experiments were performed in duplicate or triplicate, and each experiment was repeated at least three times. All values are given as the mean ± S.E.M. The significance of differences between means was evaluated using one-way analysis of variance (ANOVA). When a significant F value was found by ANOVA, Dunnett's or Scheffe's test for multiple comparisons was used to identify differences among the groups. Values were considered statistically different when the *P*-value was less than 0.05. Statistical analyses were performed using PRISM for Windows version 5.0J software (Abacus Concept, Berkeley, CA, USA).

Results

Effects of raloxifene and tamoxifen on [^{3}H]17β-E_2 binding to plasma membranes

We first examined the effects of raloxifene and tamoxifen on the specific binding of [^{3}H]17β-E_2 to plasma membranes isolated from bovine adrenal medulla. When plasma membranes were incubated with these SERMs at various concentrations, the specific binding of [^{3}H]17β-E_2 was significantly increased by raloxifene and tamoxifen at 1.0 – 10 nM (Fig. 1A) and 1.0 nM – 10 μM (except for 100 nM) (Fig. 1B), respectively, but inhibited by raloxifene at 1.0 – 10 μM (Fig. 1A). These results suggest that the SERMs interact with plasma membrane estrogen receptors to positively or negatively modulate specific [^{3}H]17β-E_2 binding.

Effects of raloxifene and tamoxifen on basal and ACh-induced ^{14}C-catecholamine synthesis from [^{14}C]tyrosine in the cells

Bovine adrenal medullary cells were incubated with 20 μM [^{14}C]tyrosine in KRP buffer in the presence or absence of various concentrations of SERMs at 37°C for 20 min. As shown in Fig. 2B, tamoxifen at 100 nM significantly increased ^{14}C-catecholamine synthesis from [^{14}C]tyrosine, but raloxifene and tamoxifen at higher concentrations (0.1 – 1.0 and 1.0 – 10 μM, respectively) inhibited it (Fig. 2: A and B). Raloxifene (100 nM) and tamoxifen (100 nM and 1.0 μM) had little effect on [^{14}C]tyrosine uptake by the cells (data not shown),

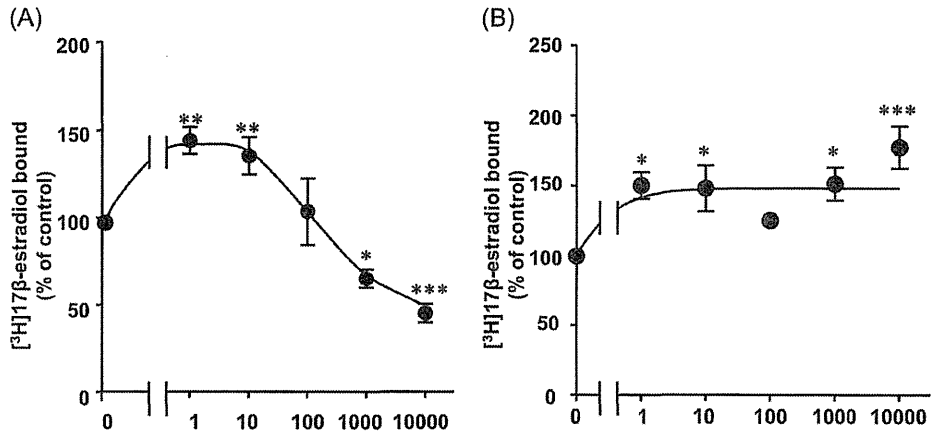

Fig. 1. Effects of raloxifene (A) and tamoxifen (B) on the specific binding of [^{3}H]17β-estradiol (17β-E_2) to plasma membranes isolated from bovine adrenal medulla. Plasma membranes (30 μg/tube) were incubated with [^{3}H]17β-E_2 (5 nM) and various concentrations of raloxifene (A) or tamoxifen (B) for 30 min at 4°C. Non-specific binding of [^{3}H]17β-E_2 was determined in the presence of 200-fold excess concentrations of 17β-E_2, and specific binding was obtained by subtracting non-specific binding from total binding. Control specific binding of [^{3}H]17β-E_2 [150 ± 15 (A) and 208 ± 36 (B) fmol/mg protein] was assigned a value of 100% and the data are expressed as % of control. Values shown are the mean ± S.E.M. of 4 experiments carried out in duplicate. $*P < 0.05$, $**P < 0.01$, and $***P < 0.001$; compared to each control.

suggesting that the SERMs do not affect tyrosine uptake by the cells. ACh (300 μM) increased ^{14}C-catecholamine synthesis, which raloxifene and tamoxifen suppressed significantly (1.0 μM and 10 – 100 μM, respectively) in a concentration-dependent manner (Fig. 2: C and D).

Effects of pretreatment with raloxifene and tamoxifen on catecholamine secretion induced by ACh in the cells

Raloxifene (1 μM) and tamoxifen (10 μM) did not significantly affect basal secretion of catecholamines (control = 2.85% ± 0.17%, raloxifene = 3.21% ± 0.41%, tamoxifen = 3.47% ± 0.23% of the total catecholamines). Stimulation of nAChR-ion channels by ACh, a physiological secretagogue, caused catecholamine secretion corresponding to 16.79% ± 0.75% of the total catecholamines in the cells (Fig. 3A). Pretreatment of cells with raloxifene (1 μM) (Fig. 3A) and tamoxifen (10 μM) (Fig. 3B) for 0, 5, 10, 20, and 30 min caused a time-dependent decrease in catecholamine secretion induced by ACh for up to 30 min, with a continuously maximal reduced level occurring at 10 min. Therefore, the effect of SERMs on catecholamine secretion was evaluated using cells pretreated with SERMs for 10 min.

We examined the effects of raloxifene (1 μM) and tamoxifen (10 μM) on catecholamine secretion induced by other secretagogues. Veratridine (100 μM), an activator of voltage-dependent Na^+ channels, or 56 mM K^+, an activator of voltage-dependent Ca^{2+} channels, caused catecholamine secretion corresponding to 24.28% ± 1.58% and 19.47% ± 1.11% of the total catecholamines, respectively (Fig. 4A). Raloxifene (1 μM) (Fig. 4A) and tamoxifen (10 μM) (Fig. 4B) had little effect on catecholamine secretion induced by veratridine and high K^+.

Concentration–inhibition curves for the effects of raloxifene or tamoxifen on ACh-induced catecholamine secretion and $^{22}Na^+$ and $^{45}Ca^{2+}$ influx

Pretreatment of cells with raloxifene (0.3, 1, 10, and 100 μM) or tamoxifen (10, 30, and 100 μM) for 10 min reduced ACh-induced secretion of catecholamines to 81.0%, 65.0%, 35.1%, and 33.0% (Fig. 5A) or to 49.0%, 43.1%, and 25.4% (Fig. 6A), respectively, of ACh alone in a concentration-dependent manner. Raloxifene suppressed ACh (300 μM)-induced $^{45}Ca^{2+}$ influx at 1.0 – 100 μM (Fig. 5B) and ACh (300 μM)-induced $^{22}Na^+$ influx at 0.3 – 100 μM (Fig. 5C). Tamoxifen also inhibited ACh-induced $^{45}Ca^{2+}$ influx (Fig. 6B) and $^{22}Na^+$ influx at 10 – 100 μM (Fig. 6C).

Inhibitory mode of raloxifene or tamoxifen on $^{22}Na^+$ influx induced by ACh

We attempted to determine whether either SERM competes with ACh for binding sites on the nAChRs. When the concentration of ACh in the incubation medium increased, the inhibition of $^{22}Na^+$ influx induced by either SERM was not overcome by increasing concentrations (10 – 300 μM) of ACh (Fig. 7: A and B), indicating that neither SERM competes with ACh for the binding sites on nAChRs.

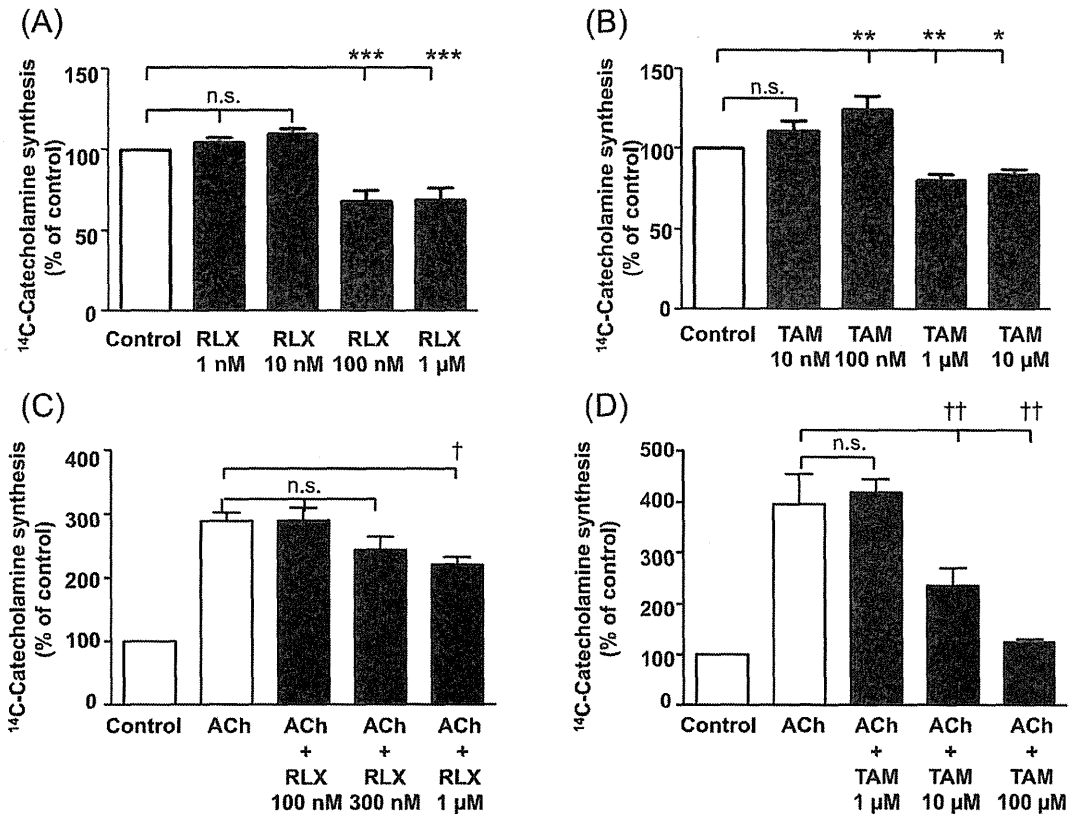

Fig. 2. Effects of raloxifene (A, C) or tamoxifen (B, D) on basal (A, B) and ACh (C, D)-induced ^{14}C-catecholamine synthesis from [^{14}C]tyrosine in the cells. Cells (4×10^6 / dish) were incubated with L-[U-^{14}C]tyrosine (20 μM, 1 μCi) and various concentrations of raloxifene (RLX) (A, C) or tamoxifen (TAM) (B, D) at 37°C for 20 min in the presence (C, D) or absence (A, B) of ACh (300 μM). ^{14}C-Labelled catechol compounds were separated by ion exchange chromatography on Duolite C-25 columns (H^+ type, 0.4×7.0 cm) and counted for radioactivity. Control ^{14}C-catecholamine synthesis [20,500 ± 3,900 (A) and 20,800 ± 6,500 (B) dpm / 4×10^6 cells / 20 min] and ACh-induced synthesis [50,600 ± 3,900 (C) and 112,000 ± 8,000 (D) dpm / 4×10^6 cells / 20 min] were assigned a value of 100% and the data are expressed as % of control or ACh. Values shown are the mean ± S.E.M. of 4 experiments carried out in duplicate. Data are expressed as the mean ± S.E.M. of 4 experiments carried out in triplicate. $^*P < 0.05$, $^{**}P < 0.01$, and $^{***}P < 0.001$; compared with each control. $^{\dagger}P < 0.05$ and $^{\dagger\dagger}P < 0.01$; compared with ACh alone.

Effects of raloxifene on ACh responses in Xenopus oocytes expressing nAChRs

The direct effect of raloxifene on ACh responses in *Xenopus* oocytes expressing rat $\alpha 4\beta 2$ nAChRs was examined. As shown in Fig. 8, raloxifene (1.0 μM) reversibly inhibited ACh-induced Na^+ currents.

Discussion

In the present study, we demonstrated the stimulatory or inhibitory effects of two SERMs, raloxifene and tamoxifen, on specific [^{3}H]17β-E_2 binding to plasma membrane estrogen receptors as well as catecholamine synthesis and secretion in bovine adrenal medullary cells.

Raloxifene and tamoxifen are allosteric modulators of plasma membrane estrogen receptors

SERMs are well-known to bind to estrogen-binding sites of classical nuclear ERs to initiate changes in formation on the ER, the dissociation of the ER from heat-shock proteins, and various gene transcriptions (2). In the present study, raloxifene at 1.0 – 10 nM and tamoxifen at 1.0 nM – 10 μM except for 100 nM rather enhanced [^{3}H]17β-E_2 binding to plasma membrane estrogen receptors, whereas raloxifene at higher concentrations (1.0 – 10 μM) inhibited it. This finding suggests that raloxifene and tamoxifen are an allosteric modulator of membrane estrogen receptors and that raloxifene at higher concentrations interferes with the specific binding of [^{3}H]17β-E_2 to membrane estrogen receptors. The

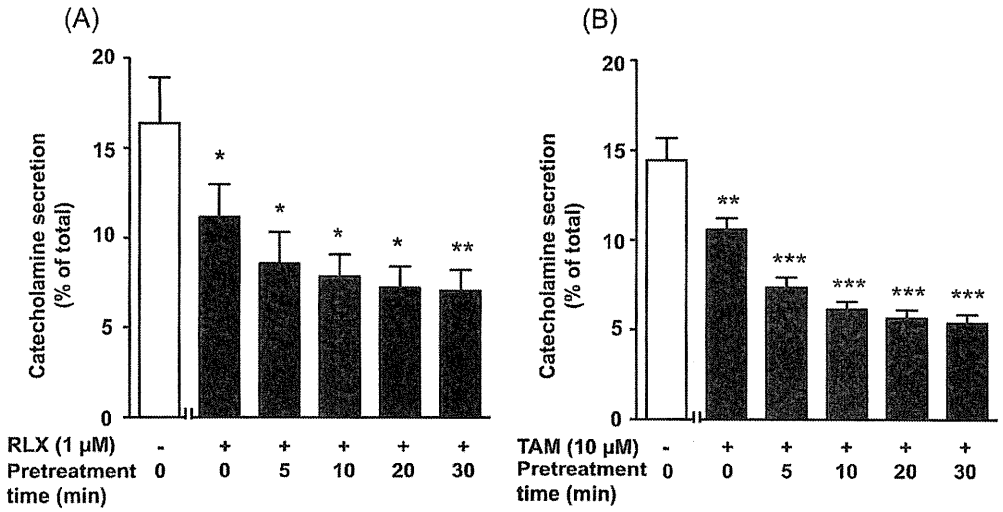

Fig. 3. Time course of pretreatment effect of raloxifene and tamoxifen on ACh-induced catecholamine secretion from the cell. After preincubation with (closed column) or without (open column) 1 μM raloxifene (RLX) (A) or 10 μM tamoxifen (TAM) (B) for the indicated period, the cells (10^6/well) were stimulated with ACh (300 μM) for 10 min at 37°C. Catecholamines secreted into the medium were measured and expressed as a percentage of the total catecholamines [7.19 ± 0.98 μg (A), 7.60 ± 0.82 μg (B)] in the cells. Data are the mean ± S.E.M. of 4 separate experiments carried out in triplicate. $^*P < 0.05$, $^{**}P < 0.01$, and $^{***}P < 0.001$; compared with ACh alone.

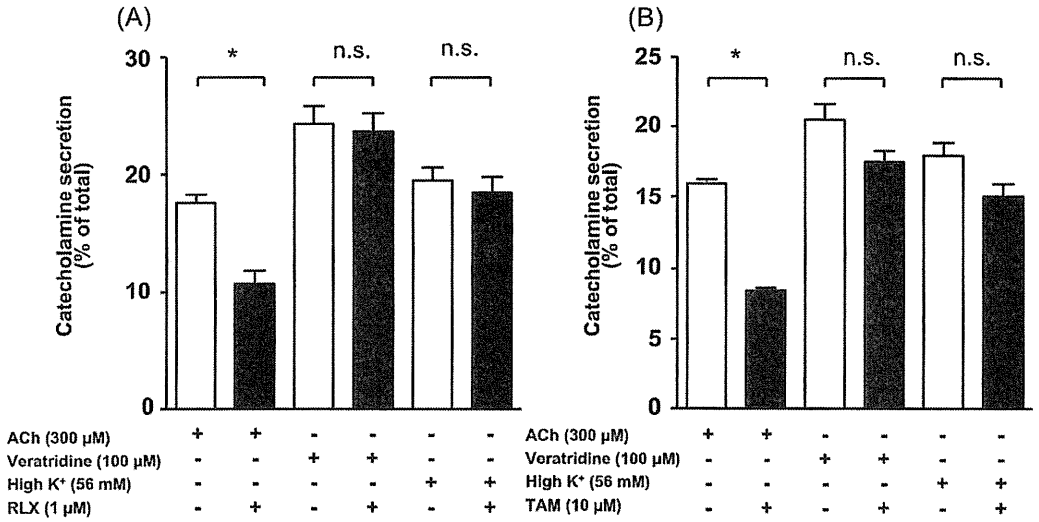

Fig. 4. Effects of raloxifene (A) or tamoxifen (B) on catecholamine secretion induced by various secretagogues. After preincubation of cells with or without raloxifene (RLX) (A) or tamoxifen (TAM) (B) for 10 min, the cells (10^6/well) were incubated with or without ACh (300 μM), veratridine (100 μM), or high concentrations of K^+ (56 mM) for another 10 min at 37°C. Catecholamines secreted into the medium were measured and expressed as a percentage of the total catecholamines [6.21 ± 1.19 μg (A), 7.28 ± 0.59 μg (B)] in the cells. Data are the mean ± S.E.M. of 4 separate experiments carried out in triplicate. $^*P < 0.05$, compared with ACh alone.

former result is similar to that of our previous data produced by ICI182,780, a pure antagonist of nuclear ER, and *p*-nonylphenol or bisphenol A, environmental estrogenic pollutants, both of which allosterically enhanced specific [^{3}H]17β-E_2 binding to plasma membrane estrogen receptors (12).

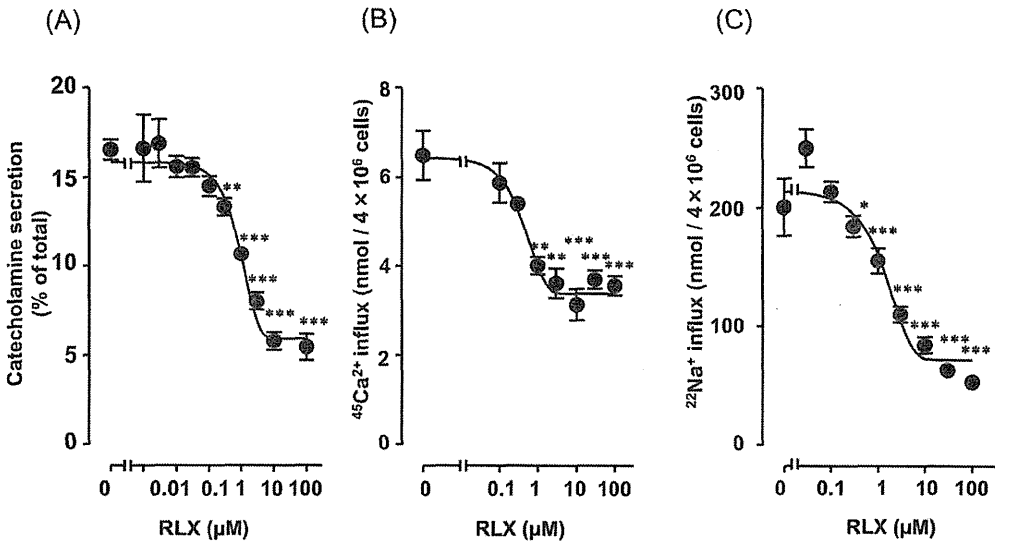

Fig. 5. Effects of various concentrations of raloxifene on ACh-induced catecholamine secretion (A), $^{45}Ca^{2+}$ influx (B), and $^{22}Na^+$ influx (C) in the cells. A) After preincubation of cells with various concentrations of raloxifene (RLX) for 10 min at 37°C, cells (10^6/well) were stimulated with ACh (300 μM) in the presence of various concentrations of raloxifene for another 10 min at 37°C. Catecholamines secreted were measured and expressed as a percentage of total catecholamines (5.01 ± 0.37 μg). B and C) After preincubation with various concentrations of raloxifene for 10 min, cells (4 × 10^6 / dish) were incubated in the presence of various concentrations of raloxifene, 300 μM ACh, 1.5 μCi of $^{45}CaCl_2$ (B), or $^{22}NaCl$ (C) for another 5 min at 37°C. $^{45}Ca^{2+}$ influx and $^{22}Na^+$ influx were measured, and expressed as nmol / 4 × 10^6 cells. Data are the mean ± S.E.M. of 4 separate experiments carried out in triplicate. $*P < 0.05$, $**P < 0.01$, and $***P < 0.001$; compared to ACh alone.

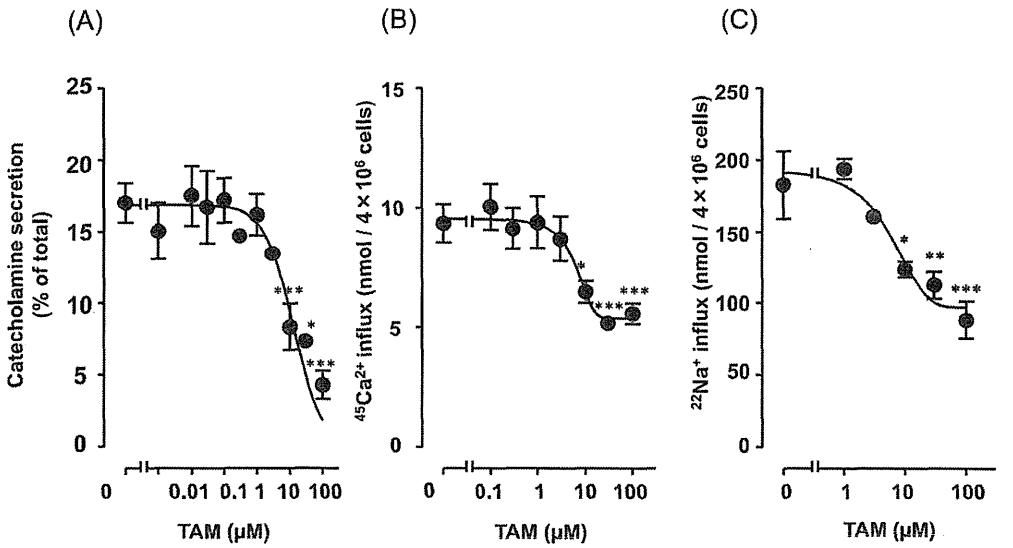

Fig. 6. Effects of various concentrations of tamoxifen on ACh-induced catecholamine secretion (A), $^{45}Ca^{2+}$ influx (B), and $^{22}Na^+$ influx (C) in the cells. A) After preincubation of cells with various concentrations of tamoxifen (TAM) for 10 min at 37°C, cells (10^6/well) were stimulated with ACh (300 μM) in the presence of various concentrations of tamoxifen for another 10 min at 37°C. Catecholamines secreted were measured and expressed as a percentage of total catecholamines (5.64 ± 0.49 μg). B and C) After preincubation with various concentrations of tamoxifen for 10 min, the cells (4 × 10^6 / dish) were incubated in the presence of various concentrations of tamoxifen, 300 μM ACh, 1.5 μCi of $^{45}CaCl_2$ (B), or $^{22}NaCl$ (C) for another 5 min at 37°C. $^{45}Ca^{2+}$ influx and $^{22}Na^+$ influx were measured, and expressed as nmol / 4 × 10^6 cells. Data are the mean ± S.E.M. of 4 separate experiments carried out in triplicate. $*P < 0.05$, $**P < 0.01$, and $***P < 0.001$; compared to ACh alone.

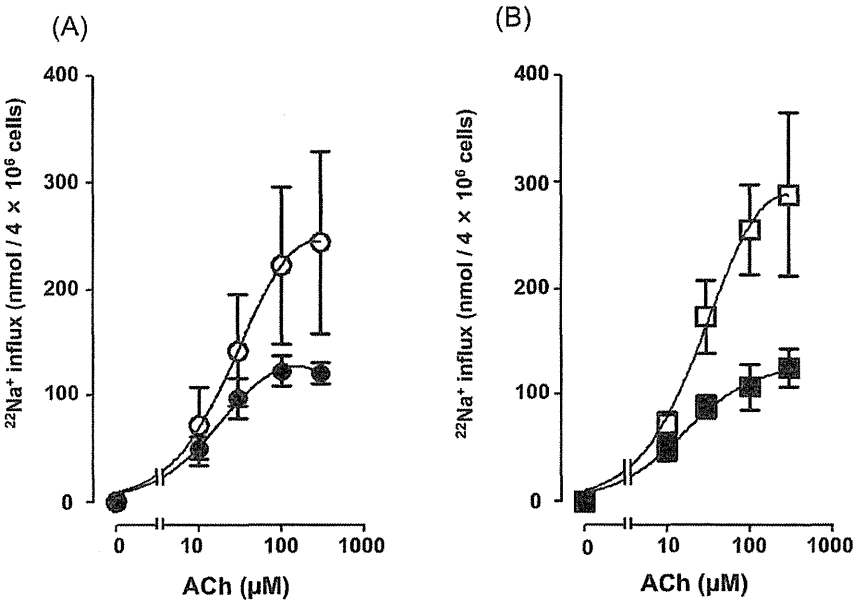

Fig. 7. Inhibitory mode of raloxifene (A) and tamoxifen (B) on $^{22}Na^+$ influx induced by ACh. After preincubation of cells with or without raloxifene (1.0 μM) and tamoxifen (10 μM) for 10 min, the cells were incubated with (closed circle) or without (open circle) raloxifene (1.0 μM) (A) and with (closed square) or without (open square) tamoxifen (10 μM) (B) in the presence of 1.5 μCi of $^{22}NaCl$ and ACh (3 – 300 μM) for 5 min at 37°C. $^{22}Na^+$ influx was measured and expressed as nmol / 4 × 10^6 cells. Data are the mean ± S.E.M. from 3 separate experiments carried out in triplicate.

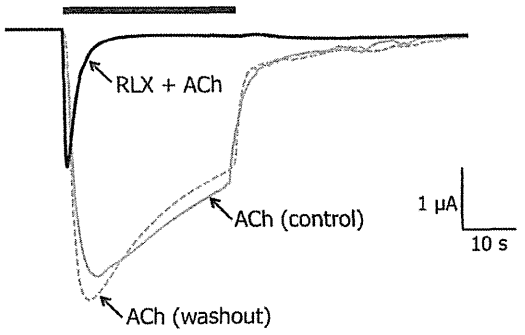

Fig. 8. Effect of raloxifene on ACh-induced response in nAChRs expressed in *Xenopus* oocytes. Representative current tracings obtained from the same *Xenopus* oocyte expressing rat $\alpha 4\beta 2$ nAChRs were superimposed, demonstrating an inhibitory effect of raloxifene (RLX, 1 μM) on the current induced by the EC_{50} of ACh. Traces represent the responses of ACh (control), in the presence of RLX (RLX + ACh), and 15-min washout [ACh (washout): dotted line]. The bar indicates the time of drug applications (ACh alone or RLX plus ACh), but it should be noted that RLX was pre-applied for 2 min before the coapplication with ACh.

Modulatory effects of raloxifene and tamoxifen on ^{14}C-catecholamine synthesis and catecholamine secretion

In bovine adrenal medullary cells, we previously reported that 17β-E_2 (12), environmental estrogenic pollutants (19), and phytoestrogens, such as daidzein (13) and resveratrol (14), stimulate catecholamine synthesis through plasma membrane estrogen receptors. A previous study reported that activation of membrane estrogen receptors increases intracellular Ca^{2+} concentrations and progesterone synthesis in rat hypothalamic astrocytes (20). In the present study, however, the stimulatory effect of tamoxifen on ^{14}C-catecholamine synthesis may not be mediated through the plasma membrane estrogen receptors because it increased basal synthesis of ^{14}C-catecholamines only at 100 nM. Furthermore, at higher concentrations raloxifene (0.1 – 1.0 μM) and tamoxifen (1.0 – 10 μM) inhibited ^{14}C-catecholamine synthesis. There was no relation between catecholamine synthesis and modulation of [^{3}H]17β-E_2 binding induced by SERMs. From these present results, it seems that the interactions of the SERMs with plasma membrane estrogen receptors are not associated with catecholamine synthesis in the cells.

Both raloxifene (1.0 μM) and tamoxifen (10 – 100 μM) suppressed ACh-induced ^{14}C-catecholamine synthesis in a concentration-dependent manner. We previously reported that ACh activates nAChR-ion channels, thereby inducing Na^+ influx and then Ca^{2+} influx as well as catecholamine synthesis (10) and secretion (11). In the present study, raloxifene and tamoxifen both preferentially inhibited catecholamine secretion mediated through nAChRs but neither did so through voltage-dependent Na^+ channels or voltage-dependent Ca^{2+} channels. The present results were partially consistent with those of a previous report (7) that raloxifene at micromolar concentrations inhibited catecholamine output elicited by ACh or high potassium in perfused rat adrenal glands and cultured bovine adrenal medullary cells. In the present study, both SERMs suppressed ACh-induced $^{45}Ca^{2+}$

influx and $^{22}Na^+$ influx in a concentration-dependent manner, similar to their suppression of catecholamine secretion and synthesis. It is likely that raloxifene and tamoxifen suppress ACh-induced catecholamine synthesis and secretion primarily by inhibiting Na^+ influx through nAChR-ion channels and subsequent Ca^{2+} influx through voltage-dependent Ca^{2+} channels.

We further investigated the inhibitory mechanisms underlying the effects of raloxifene and tamoxifen on nAChR-ion channels. Increased concentrations of ACh did not overcome the inhibitory effects of the SERMs on ACh-induced $^{22}Na^+$ influx, suggesting that the SERMs act on the sites differently than they act on ACh binding sites of nAChR-ion channels. We confirmed that raloxifene directly and reversibly suppressed ACh-induced Na^+ current in *Xenopus* oocytes expressing rat $\alpha4\beta2$ nAChR.

Pharmacological significance of the effects of the SERMs on catecholamine synthesis and secretion

The pharmacokinetic properties of raloxifene and tamoxifen in postmenopausal women and in women with breast cancer showed that the maximum plasma concentrations of raloxifene and tamoxifen were 2 – 3 nM and 20 – 330 nM, respectively, during clinical treatments (21, 22). Tamoxifen, however, is reported to accumulate in tissues, resulting in 100-fold higher concentrations than in plasma after repeated administration of the drug during long-term treatment for breast cancer (23). Therefore, the concentrations of raloxifene and tamoxifen used in the present study should be high, compared to those plasma therapeutic concentrations, but they might be clinically relevant in the tissues.

Several lines of evidence have shown that the SERMs have both potentially adverse (24) and beneficial effects on brain functions such as cognition (25, 26) and neuroprotection (27). Indeed, raloxifene is reported to induce neurite outgrowth in estrogen receptor–positive PC12 cells (28). In the present study, we demonstrated that low concentration of tamoxifen (100 nM) stimulates basal catecholamine synthesis, whereas at high concentrations, it inhibits basal and ACh-induced catecholamine synthesis and secretion. On the basis of the present results, it would be hypothesized that the SERMs negatively or positively modulate the functions of central noradrenergic or dopaminergic neurons, depending on their concentrations, by changing the synthesis and release of each neurotransmitter. To confirm this possibility, further in vivo studies are required in the near future.

In summary, we demonstrated that two SERMs, raloxifene and tamoxifen, allosterically interact with plasma membrane estrogen receptors, whereas at high concentrations each of them inhibits catecholamine synthesis and secretion induced by ACh in adrenal medullary cells and probably in peripheral and central sympathetic neurons.

Acknowledgments

This research was supported, in part, by Grants-in-Aid (23617035, 23590159, 23617036, and 24890286) for Scientific Research (C) from the Japan Society for the Promotion of Science. We are grateful to Dr. James A. Patrick (Division of Neuroscience, Baylor College of Medicine, Houston, TX, USA) for providing rat nAChR subunit cDNAs used in this study.

Conflicts of Interest

The authors have no conflict of interest to report.

References

1 MacGregor JI, Jordan VC. Basic guide to the mechanisms of antiestrogen action. Pharmacol Rev. 1998;50:151–196.
2 Smith CL, O'Malley BW. Coregulator function: a key to understanding tissue specificity of selective receptor modulators. Endocr Rev. 2004;25:45–71.
3 Jordan VC, Gapstur S, Morrow M. Selective estrogen receptor modulation and reduction in risk of breast cancer, osteoporosis, and coronary heart disease. J Natl Cancer Inst. 2001;93:1449–1457.
4 Mauvais-Jarvis F, Clegg DJ, Hevener AL. The role of estrogens in control of energy balance and glucose homeostasis. Endocr Rev. 2013;34:309–338.
5 Yamaguchi K, Honda H, Wakisaka C, Tohei A, Kogo H. Effects of phytoestrogens on acetylcholine- and isoprenaline-induced vasodilation in rat aorta. Jpn J Pharmacol. 2001;87:67–73.
6 Nakazawa K, Ohno Y. Block by phytoestrogens of recombinant human neuronal nicotinic receptors. J Pharmacol Sci. 2003;93:118–121.
7 Machado JD, Alonso C, Morales A, Gomez JF, Borges R. Nongenomic regulation of the kinetics of exocytosis by estrogens. J Pharmacol Exp Ther. 2002;301:631–637.
8 Kim YJ, Hur EM, Park TJ, Kim KT. Nongenomic inhibition of catecholamine secretion by 17β-estradiol in PC12 cells. J Neurochem. 2000;74:2490–2496.
9 Weiner N. Regulation of norepinephrine biosynthesis. Annu Rev Pharmacol. 1970;10:273–290.
10 Yanagihara N, Wada A, Izumi F. Effects of α_2-adrenergic agonists on carbachol-stimulated catecholamine synthesis in cultured bovine adrenal medullary cells. Biochem Pharmacol. 1987;36:3823–3828.
11 Wada A, Takara H, Izumi F, Kobayashi H, Yanagihara N. Influx of ^{22}Na through acetylcholine receptor-associated Na channels: relationship between ^{22}Na influx, ^{45}Ca influx and secretion of catecholamines in cultured bovine adrenal medulla cells. Neuroscience. 1985;15:283–292.
12 Yanagihara N, Liu M, Toyohira Y, Tsutsui M, Ueno S, Shinohara Y, et al. Stimulation of catecholamine synthesis through unique estrogen receptors in the bovine adrenomedullary plasma membrane by 17β-estradiol. Biochem Biophys Res Commun.

2006;339:548–553.
13 Liu M, Yanagihara N, Toyohira Y, Tsutsui M, Ueno S, Shinohara Y. Dual effects of daidzein, a soy isoflavone, on catecholamine synthesis and secretion in cultured bovine adrenal medullary cells. Endocrinology. 2007;148:5348–5354.
14 Shinohara Y, Toyohira Y, Ueno S, Liu M, Tsutsui M, Yanagihara N. Effects of resveratrol, a grape polyphenol, on catecholamine secretion and synthesis in cultured bovine adrenal medullary cells. Biochem Pharmacol. 2007;74:1608–1618.
15 Yanagihara N, Isosaki M, Ohuchi T, Oka M. Muscarinic receptor-mediated increase in cyclic GMP level in isolated bovine adrenal medullary cells. FEBS Lett. 1979;105:296–298.
16 Yanagihara N, Oishi Y, Yamamoto H, Tsutsui M, Kondoh J, Sugiura T, et al. Phosphorylation of chromogranin A and catecholamine secretion stimulated by elevation of intracellular Ca^{2+} in cultured bovine adrenal medullary cells. J Biol Chem. 1996; 271:17463–17468.
17 Ueno S, Tsutsui M, Toyohira Y, Minami K, Yanagihara N. Sites of positive allosteric modulation by neurosteroids on ionotropic γ-aminobutyric acid receptor subunits. FEBS Lett. 2004;566: 213–217.
18 Horishita T, Ueno S, Yanagihara N, Sudo Y, Uezono Y, Okura D, et al. Inhibition by pregnenolone sulphate, a metabolite of the neurosteroid pregnenolone, of voltage-gated sodium channels expressed in *Xenopus* oocytes. J Pharmacol Sci. 2012;120: 54–58.
19 Yanagihara N, Toyohira Y, Ueno S, Tsutsui M, Utsunomiya K, Liu M, et al. Stimulation of catecholamine synthesis by environmental estrogenic pollutants. Endocrinology. 2005;146:265–272.
20 Kuo J, Hamid N, Bondar G, Prossnitz ER, Micevych P. Membrane estrogen receptors stimulate intracellular calcium release and progesterone synthesis in hypothalamic astrocytes. J Neurosci. 2010;30:12950–12957.
21 Wada T, Koyama H, Takahashi Y, Nishizawa Y, Iwanaga T, Aoki Y, et al. [Tamoxifen therapy in locally advanced primary and recurrent breast cancer (author's transl)]. Nihon Gan Chiryo Gakkai Shi. 1979;14:819–824. (text in Japanese)
22 Traina TA, Poggesi I, Robson M, Asnis A, Duncan BA, Heerdt A, et al. Pharmacokinetics and tolerability of exemestane in combination with raloxifene in postmenopausal women with a history of breast cancer. Breast Cancer Res Treat. 2008;111: 377–388.
23 Lien EA, Solheim E, Ueland PM. Distribution of tamoxifen and its metabolites in rat and human tissues during steady-state treatment. Cancer Res. 1991;51:4837–4844.
24 Espeland MA, Shumaker SA, Limacher M, Rapp SR, Bevers TB, Barad DH, et al. Relative effects of tamoxifen, raloxifene, and conjugated equine estrogens on cognition. J Womens Health (Larchmt). 2010;19:371–379.
25 Yaffe K, Krueger K, Cummings SR, Blackwell T, Henderson VW, Sarkar S, et al. Effect of raloxifene on prevention of dementia and cognitive impairment in older women: the Multiple Outcomes of Raloxifene Evaluation (MORE) randomized trial. Am J Psychiatry. 2005;162:683–690.
26 Legault C, Maki PM, Resnick SM, Coker L, Hogan P, Bevers TB, et al. Effects of tamoxifen and raloxifene on memory and other cognitive abilities: cognition in the study of tamoxifen and raloxifene. J Clin Oncol. 2009;27:5144–5152.
27 Kuo YM, Chen HH, Shieh CC, Chuang KP, Cherng CG, Yu L. 4-Hydroxytamoxifen attenuates methamphetamine-induced nigrostriatal dopaminergic toxicity in intact and gonadetomized mice. J Neurochem. 2003;87:1436–1443.
28 Nilsen J, Mor G, Naftolin F. Raloxifene induces neurite outgrowth in estrogen receptor positive PC12 cells. Menopause. 1998;5:211–216.

Lidocaine Preferentially Inhibits the Function of Purinergic P2X7 Receptors Expressed in *Xenopus* Oocytes

Dan Okura, MD,* Takafumi Horishita, MD, PhD,* Susumu Ueno, MD, PhD,† Nobuyuki Yanagihara, PhD,‡ Yuka Sudo, PhD,§ Yasuhito Uezono, MD, PhD,‖ Tomoko Minami, MD,* Takashi Kawasaki, MD, PhD,* and Takeyoshi Sata, MD, PhD*

BACKGROUND: Lidocaine has been widely used to relieve acute pain and chronic refractory pain effectively by both systemic and local administration. Numerous studies reported that lidocaine affects several pain signaling pathways as well as voltage-gated sodium channels, suggesting the existence of multiple mechanisms underlying pain relief by lidocaine. Some extracellular adenosine triphosphate (ATP) receptor subunits are thought to play a role in chronic pain mechanisms, but there have been few studies on the effects of lidocaine on ATP receptors. We studied the effects of lidocaine on purinergic P2X3, P2X4, and P2X7 receptors to explore the mechanisms underlying pain-relieving effects of lidocaine.

METHODS: We investigated the effects of lidocaine on ATP-induced currents in ATP receptor subunits, P2X3, P2X4, and P2X7 expressed in *Xenopus* oocytes, by using whole-cell, two-electrode, voltage-clamp techniques.

RESULTS: Lidocaine inhibited ATP-induced currents in P2X7, but not in P2X3 or P2X4 subunits, in a concentration-dependent manner. The half maximal inhibitory concentration for lidocaine inhibition was 282 ± 45 μmol/L. By contrast, mepivacaine, ropivacaine, and bupivacaine exerted only limited effects on the P2X7 receptor. Lidocaine inhibited the ATP concentration–response curve for the P2X7 receptor via noncompetitive inhibition. Intracellular and extracellular *N*-(2,6-dimethylphenylcarbamoylmethyl) triethylammonium bromide (QX-314) and benzocaine suppressed ATP-induced currents in the P2X7 receptor in a concentration-dependent manner. In addition, repetitive ATP treatments at 5-minute intervals in the continuous presence of lidocaine revealed that lidocaine inhibition was use-dependent. Finally, the selective P2X7 receptor antagonists Brilliant Blue G and AZ11645373 did not affect the inhibitory actions of lidocaine on the P2X7 receptor.

CONCLUSIONS: Lidocaine selectively inhibited the function of the P2X7 receptor expressed in *Xenopus* oocytes. This effect may be caused by acting on sites in the ion channel pore both extracellularly and intracellularly. These results help to understand the mechanisms underlying the analgesic effects of lidocaine when it is administered locally at least. (Anesth Analg 2015;120:597–605)

Systemic administration of lidocaine has been used to relieve neuropathic pain, including that from malignant and nonmalignant disorders.[1,2] Abnormal expression of voltage-gated sodium channels in both injured and neighboring areas correlates with ectopic activity[3] that has been proposed as a mechanism underlying neuropathic pain,[4] suggesting the role of blockade of specific sodium channels by intravenous lidocaine to produce neuropathic pain relief.[5] However, lidocaine has other several beneficial effects in some clinical situations such as postoperative pain relief by epidural administration, stimulation of bowel function after colon surgery,[6] and topical anesthesia in addition to properties including antithrombotic[7] and anti-inflammatory actions,[8] which are potentially important during the perioperative period. These multiple effects of lidocaine indicate that there may be mechanisms other than sodium channel blockade. Moreover, the difference of effective concentrations between intravenous and epidural administration also supports this possibility. Indeed, several reports demonstrated that lidocaine affects other pain signaling pathways,[9] receptors, and ion channels including Gq protein,[10] potassium channels,[11] and calcium channels.[12]

Extracellular adenosine triphosphate (ATP) is a neurotransmitter acting through ATP receptors, which are classified as ligand-gated ion channels (P2X receptors) and G-protein–coupled receptors (P2Y receptors). Seven P2X (P2X1–7) and eight P2Y (P2Y1, P2Y2, P2Y4, P2Y6, P2Y11–14) subunits have been identified.[13] They are distributed in multiple organs and have important roles in various physiologic functions.[14,15] Recently, specific receptor subunits have been shown to be involved in various pathologic conditions, including brain ischemia, pain, inflammation,

From the *Department of Anesthesiology, School of Medicine, University of Occupational and Environmental Health, Yahatanishiku, Kitakyushu, Fukuoka, Japan; †Department of Occupational Toxicology, Institute of Industrial Ecological Sciences, University of Occupational and Environmental Health, Yahatanishiku, Kitakyushu, Fukuoka, Japan; ‡Department of Pharmacology, School of Medicine, University of Occupational and Environmental Health, Yahatanishiku, Kitakyushu, Fukuoka, Japan; §Department of Molecular Pathology and Metabolic Disease, Faculty of Pharmaceutical Sciences, Tokyo University of Science, Noda, Chiba, Japan; and ‖Cancer Pathophysiology Division, National Cancer Center Research Institute, Chuouku, Tokyo, Japan.

Accepted for publication October 24, 2014.

Funding: This study was supported by a Grant-in-Aid for Scientific Research from Japan Society for the Promotion of Science, 22591756 (to TS).

The authors declare no conflicts of interest.

Address correspondence to Takafumi Horishita, MD, PhD, Department of Anesthesiology, School of Medicine, University of Occupational and Environmental Health, 1-1 Iseigaoka, Yahatanishiku, Kitakyushu, Fukuoka 807–8555, Japan. Address e-mail to thori@med.uoeh-u.ac.jp.

DOI: 10.1213/ANE.0000000000000585

osteoporosis, spinal cord injury, and bladder dysfunction; therefore, these receptors are considered to be potential therapeutic targets.[16–19] It is especially suggested that several subunits including P2X3, P2X4, and P2X7 receptors, which are distributed in pain pathways within the nervous system, are involved in chronic pain mechanisms.[20]

P2X3 receptors, which are mainly distributed in sensory neurons such as dorsal root ganglia, have been shown to be involved in the mechanism of neuropathic pain by demonstrating that intrathecal treatment with P2X3 antisense oligonucleotide decreased nociceptive behavior in a model of chronic inflammation and reduced mechanical allodynia in a rat model of neuropathic pain.[21] P2X4 receptors are widely expressed in the brain, spinal cord, autonomic and sensory ganglia, and microglia. Several reports demonstrated that upregulation of P2X4 receptors in activated microglia located in the dorsal horn of the spinal cord contributes to neuropathic pain.[22] P2X7 receptors are expressed on cells of the immune system as well as glial cells. In addition, inflammatory and neuropathic hypersensitivities in response to mechanical and thermal stimuli were completely absent in mice lacking P2X7 receptors,[23] suggesting a role of P2X7 receptors in pain modulation.

Although previous reports have demonstrated the effects of some general anesthetics, ethanol, and antidepressants on P2X receptors,[24–28] no studies have investigated whether local anesthetics act on these receptors. Therefore, we investigated the effects of lidocaine and other local anesthetics on P2X3, P2X4, and P2X7 receptors to explore the mechanisms underlying the pain-relieving effects of lidocaine.

METHODS

This study was approved by the Animal Research Committee of the University of Occupational and Environmental Health, Kitakyushu, Japan.

Drugs

All chemicals, including ATP disodium salt, lidocaine hydrochloride, ropivacaine hydrochloride, bupivacaine hydrochloride, benzocaine, *N*-(2,6-dimethylphenylcarbamoylmethyl) triethylammonium bromide (QX-314), AZ11645373, and Brilliant Blue G (BBG), were purchased from Sigma-Aldrich (St. Louis, MO).

Plasmids

All plasmids including human P2X3, P2X4, and P2X7 receptor complementary DNA (cDNA) were purchased from OriGene Technologies (Rockville, MD).

cRNA Preparation and Oocyte Injection

After double digestion of cDNA with *Sac*I and *Sma*I (P2X3 receptor) or linearization with *Sac*I (P2X4 and P2X7 receptors), complementary RNAs (cRNA) were transcribed using T7 RNA polymerase using an mMESSAGE mMACHINE kit (Ambion, Austin, TX). Adult female *Xenopus laevis* frogs were obtained from Kyudo (Saga, Japan). *X. laevis* oocytes and cRNA microinjection were prepared and performed as described previously.[29,30] In brief, stage IV to VI oocytes were manually isolated from a removed portion of ovary. Next, oocytes were treated with collagenase (0.5 mg/mL) for 10 minutes and placed in modified Barth solution (88 mmol/L NaCl, 1 mmol/L KCl, 2.4 mmol/L $NaHCO_3$, 10 mmol/L HEPES, 0.82 mmol/L $MgSO_4$, 0.33 mmol/L $Ca[NO_3]_2$, and 0.91 mmol/L $CaCl_2$, adjusted to pH 7.5), supplemented with 10,000 U penicillin, 50 mg gentamicin, 90 mg theophylline, and 220 mg/L sodium pyruvate (incubation medium). cRNAs of P2X receptors were injected (total volume was 0.5–20 ng/50 nL) into *Xenopus* oocytes. Injected oocytes were incubated at 19°C in incubation medium, and 2 to 6 days after injection, the cells were used for electrophysiologic recordings.

Electrophysiologic Recordings

All electrical recordings were performed at room temperature (20–23°C). Oocytes were placed in a 100-μL recording chamber and perfused at 2 mL/min with extracellular Ringer's solution (110 mmol/L NaCl, 2.5 mmol/L KCl, 10 mmol/L HEPES, 1.8 mmol/L $BaCl_2$, pH 7.5) using a peristaltic pump (World Precision Instruments, Sarasota, FL). Ca^{2+} in the solution was replaced with Ba^{2+} to prevent the activation of Ca^{2+}-dependent Cl^- channels.[31,32] Recording electrodes were prepared with borosilicate glass capillary tubing using a puller (PP-830; Narishige, Tokyo, Japan); microelectrodes had a resistance of 1 to 3 MΩ when filled with 3 mol/L KCl. Whole-cell voltage clamp was achieved using these two electrodes with a Warner Instruments model OC-725C system (Warner, Hamden, CT) at −70 mV. Local anesthetics, BBG, and ATP disodium salt stocks were prepared and diluted before adding to the bath solution. AZ11645373 stocks were prepared in dimethylsulfoxide and diluted in bath solution to a final dimethylsulfoxide concentration not exceeding 0.05%. We measured the peak of the transient inward current in response to ATP that was applied for 20 seconds. Local anesthetics were preapplied for 2 minutes to allow a complete change of bath solution.

To characterize the inhibitory effect of lidocaine on P2X7 receptors, we measured ATP-induced currents at 10 μmol/L to 5 mmol/L in the presence or absence of 300 μmol/L lidocaine. The quaternary local anesthetic QX-314, which is 99.9% permanently charged and does not penetrate the cell membrane, was either injected directly into oocytes or applied outside the cell to identify whether it acts intracellularly or extracellularly. QX-314 (50 nL of 5 mmol/L diluted in 150 mmol/L KCl) was injected into oocytes to result in an intracellular concentration of approximately 500 μmol/L although, in practice, the intracellular concentration in each oocyte may be variable because the oocytes are heavily compartmentalized. Control cells were injected with 150 mmol/L KCl. Recordings were performed 10 minutes after injection. To investigate the potential use-dependent effects of lidocaine, ATP was applied at 5-minute intervals in the continuous presence of 100 μmol/L lidocaine for 30 minutes. The results are expressed as percentages of control responses.

Statistical Analyses

GraphPad Prism software (GraphPad Software, San Diego, CA) was used to conduct the statistical analysis. All values are presented as means ± SEM. The *n* values refer to the number of oocytes examined. Each experiment was performed with oocytes from at least two frogs.

The concentration–response curves for the ATP-induced peak current were fitted using the logistic function: $I = I_{min} + (I_{max} - I_{min})/[1 + (EC_{50}/A)^n]$, where I is the response induced by ATP concentration, I_{min} is the minimal response, I_{max} is the maximal response, EC_{50} is the half maximal effective concentration, A is the concentration of ATP, and n is the Hill coefficient. Differences were evaluated statistically using unpaired, two-tailed t test and one-way analysis of variance followed by Dunnett multiple comparison test, where the objective is to identify groups whose means are significantly different from the mean of a selected "reference group," in our case, no treatment with local anesthetics, or Tukey multiple comparison test, where the mean of each group is compared with the mean of every other group. Hill coefficient, half maximal inhibitory concentration (IC_{50}), and EC_{50} values were also calculated. Values of $P < 0.01$ were taken as showing a significant difference.

RESULTS

Effects of Lidocaine on Peak ATP-Induced Inward Currents in the P2X3, P2X4, and P2X7 Receptors

We determined the ATP concentration–response relation under our experimental conditions for P2X3, P2X4, and P2X7 receptors. Nonlinear regression analyses of the curves yielded the EC_{50} for ATP and slope variables (Hill coefficient) of 2.3 ± 0.8 μmol/L and 0.74 ± 0.1 in oocytes expressing P2X3 receptors, 10.8 ± 3.3 μmol/L and 0.69 ± 0.2 in oocytes expressing P2X4 receptors, and 1.2 ± 0.1 mmol/L and 3.7 ± 0.9 in oocytes expressing P2X7 receptors, respectively (Fig. 1). Based on these results, the effects of lidocaine on ATP-induced currents were examined at an ATP concentration of 2 μmol/L for P2X3 receptor, 10 μmol/L for P2X4 receptor, and 1 mmol/L for P2X7 receptor. Figure 2B shows concentration–response relations of lidocaine-mediated inhibition on ATP-induced currents in three receptors. Lidocaine inhibited the currents in a concentration-dependent manner in oocytes expressing P2X7 receptor; the IC_{50} value of lidocaine for ATP-induced currents and the slope were 282 ± 45 μmol/L and 0.72 ± 0.07, respectively (Table 1). These inhibitory effects were significant at concentrations of lidocaine ≥30 μmol/L (Fig. 2B). By contrast, the inhibitory effects of lidocaine on the P2X3 and P2X4 receptors were limited. Specifically, only a high concentration of 10 mmol/L lidocaine significantly suppressed ATP-induced currents to 68 ± 6% and 71 ± 6% of the control in oocytes expressing P2X3 and P2X4 receptors, respectively (Fig. 2B).

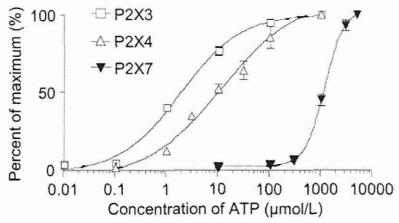

Figure 1. Concentration–response curves for adenosine triphosphate (ATP)-induced currents in *Xenopus* oocytes expressing P2X3, P2X4, and P2X7 receptors. Oocytes were voltage clamped at −70 mV. ATP (10 nmol/L to 1 mmol/L for P2X3; 100 nmol/L to 1 mmol/L for P2X4; and 10 μmol/L to 5 mmol/L for P2X7) was applied for 20 seconds, and peak current was measured. Values are the mean ± SEM (n = 6).

Effects of Other Local Anesthetics on the P2X7 Receptor

We next examined the effects of other local anesthetics including mepivacaine, ropivacaine, and bupivacaine on ATP-induced currents in oocytes expressing P2X7 receptor because lidocaine inhibited this receptor most strongly. Although mepivacaine suppressed ATP-induced currents in a concentration-dependent manner, the inhibitory effects were less than those of lidocaine with the IC_{50} value and slope variable of 6.0 ± 0.06 mmol/L and 0.62 ± 0.06, respectively. This suggests that the inhibitory potency of mepivacaine was one-twentieth of that of lidocaine (Fig. 3, Table 1). By contrast, ropivacaine and bupivacaine had little effect on ATP-induced currents (Fig. 3).

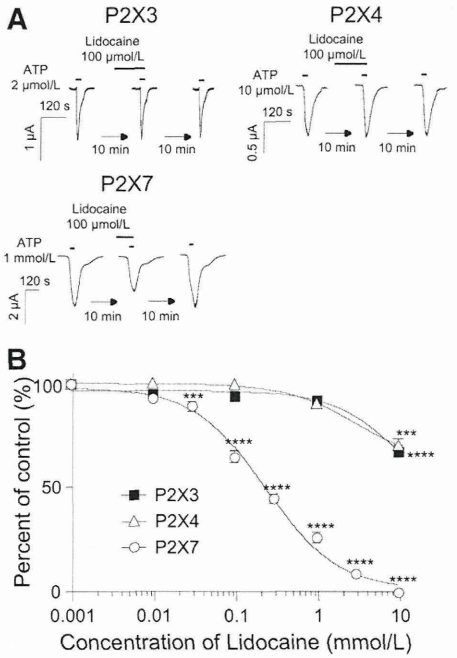

Figure 2. Effects of lidocaine on the adenosine triphosphate (ATP)-induced currents in *Xenopus* oocytes expressing P2X3, P2X4, and P2X7 receptors. A, Representative traces from oocytes expressing P2X3, P2X4, and P2X7 receptors in both the absence and presence of 100 μmol/L lidocaine. P2X3, P2X4, and P2X7 receptors were activated by 2 μmol/L, 10 μmol/L, and 1 mmol/L of ATP, respectively. ATP was applied for 20 seconds with or without pretreatment for 2 minutes with 100 μmol/L lidocaine. The currents of lidocaine-treated oocytes were recorded 10 minutes after recording the control currents, and the washout currents were obtained 10 minutes after lidocaine treatment. B, Concentration–response curves for the inhibitory effects of lidocaine on ATP-induced currents in P2X3, P2X4, and P2X7 receptors. The peak current amplitude in the presence of lidocaine was normalized to that of the control and the effects are expressed as percentages of the control. Lidocaine inhibited ATP-induced currents in oocytes expressing both P2X3 and P2X4 receptors at only a high concentration of 10 mmol/L. In contrast, lidocaine suppressed ATP-induced currents in oocytes expressing P2X7 concentration dependently, and it reduced those currents to 93 ± 4%, 89 ± 5%, 65 ± 8%, 45 ± 6%, 26 ± 7%, and 9 ± 2% of control at 10 μmol/L, 30 μmol/L, 100 μmol/L, 300 μmol/L, 1 mmol/L, and 3 mmol/L, respectively. Data are presented as means ± SEM (n = 6). Hill coefficient and half maximal inhibitory concentration (IC_{50}) values were calculated using GraphPad Prism. ***$P < 0.001$ and ****$P < 0.0001$ compared with the control (one-way analysis of variance followed by Dunnett post hoc test).

Table 1. Effects of Lidocaine, Mepivacaine, QX-314, and Benzocaine on IC_{50} Value and Hill Coefficient Calculated from the Concentration–Response Curves Shown in Figures 3 and 5

	Lidocaine	Mepivacaine	QX-314	Benzocaine
IC_{50} (μmol/L)	282 ± 45	6020 ± 61	500 ± 75	1560 ± 39
Hill coefficient	0.72 ± 0.07	0.62 ± 0.06	0.36 ± 0.03	0.88 ± 0.07

IC_{50} = half maximal inhibitory concentration; QX-314 = (*N*-[2,6-dimethylphenylcarbamoylmethyl] triethylammonium bromide).

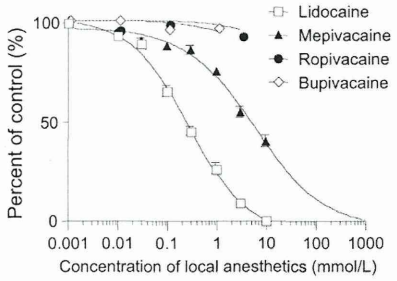

Figure 3. Concentration–response curves for inhibitory effects of local anesthetics including lidocaine, mepivacaine, ropivacaine, and bupivacaine on adenosine triphosphate–induced currents in P2X7 receptors. The peak current amplitude in the presence of local anesthetics was normalized to that of the control and the effects are expressed as percentages of the control. Data are presented as means ± SEM (n = 6). Hill coefficient and half maximal inhibitory concentration (IC_{50}) values were calculated using GraphPad Prism.

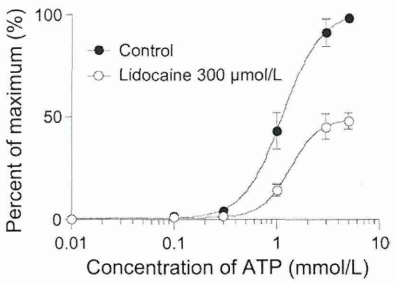

Figure 4. Characterization of the inhibitory effects of lidocaine on adenosine triphosphate (ATP)-induced currents in oocytes expressing P2X7 receptor. We measured the currents induced by 10 μmol/L to 5 mmol/L ATP in the absence and presence of 300 μmol/L lidocaine. Lidocaine did not change the half maximal effective concentration (EC_{50}) value and the the slope variable (hill coefficient) (control, 1.2 ± 0.1 mmol/L and 3.7 ± 0.9; lidocaine, 1.4 ± 0.2 mmol/L and 4.8 ± 1.1), however, it significantly reduced the maximal response (E_{max}) value to 49 ± 4% of control (P < 0.0001; 99% confidence interval, −65.7 to −35.1). Data are presented as means ± SEM (n = 6). Hill coefficient, EC_{50}, and E_{max} values were calculated using GraphPad Prism. Data were statistically evaluated by unpaired t test (two-tailed) using the same software.

Characterization of the Inhibitory Effects of Lidocaine on the P2X7 Receptor

To determine whether lidocaine competes with ATP for the P2X7 receptor, we next investigated the effects of 300 μmol/L lidocaine on the ATP concentration–response curve. ATP-induced currents at concentrations of 10 μmol/L to 5 mmol/L were measured in the absence and presence of lidocaine. As shown in Figure 4, lidocaine-mediated inhibition was not overcome by increasing the ATP concentration. In addition, lidocaine significantly reduced the E_{max} value (maximal response) of the ATP concentration–response curve to 49% ± 4% (P < 0.0001; 99% confidence interval [CI], −65.7 to −35.1). The EC_{50} and slope variables in the absence and presence of lidocaine were 1.2 ± 0.1 mmol/L and 3.7 ± 0.9, and 1.4 ± 0.2 mmol/L and 4.8 ± 1.1, respectively. Thus, lidocaine significantly suppressed E_{max} without significantly changing EC_{50} (P = 0.385; 99% CI, −0.279 to 0.665) and slope variables (P = 0.483; 99% CI, −2.165 to 4.268), suggesting noncompetitive inhibition.

Effects of Charged and Uncharged Local Anesthetics on the P2X7 Receptor

We next assessed the effects of QX-314, which is a permanently charged and non–membrane-permeable lidocaine analog, on the P2X7 receptor. When applied extracellularly, QX-314 inhibited ATP-induced currents in a concentration-dependent manner; the IC_{50} value and slope variable were 500 ± 75 μmol/L and 0.36 ± 0.03, respectively (Fig. 5B, Table 1). Moreover, intracellular QX-314 injection also significantly suppressed ATP-activated currents to 51 ± 9% of the control, whereas injected 150 mmol/L KCl had no effect (112 ± 11% of the control) (Fig. 5C). These results suggest that QX-314 can act on the P2X7 receptor both extracellularly and intracellularly, and the charged lidocaine can suppress the function of P2X7. Therefore, we investigated whether charge is required for the inhibitory actions of local anesthetics on the P2X7 receptor by measuring the effects of benzocaine, a local anesthetic that is almost completely uncharged and highly membrane permeable. Benzocaine suppressed the response to ATP in a concentration-dependent manner with the IC_{50} value and the slope variable of 1.6 ± 0.04 mmol/L and 0.88 ± 0.07, respectively (Fig. 5B, Table 1). These data suggest that both charged and uncharged local anesthetics can suppress P2X7 receptor function although it remains unclear whether benzocaine acts intracellularly or extracellularly.

Analyzing the Use Dependency of Lidocaine-Mediated Inhibition of the P2X7 Receptor

We assessed whether the effects of lidocaine on the P2X7 receptor were use-dependent because local anesthetics exhibit use-dependent block of voltage-gated sodium channel function, ATP was applied to oocytes at 5-minute intervals in the absence or continuous presence of 100 μmol/L lidocaine for 30 minutes (Fig. 6A). In the continuous presence of lidocaine, the response to the second application of ATP (after 5 minutes) was significantly reduced to 66 ± 3% of the current induced by the first application (0 minute), and the inhibitory effect of the seventh application (30 minutes) was similar to that of the second application (5 minutes) (Fig. 6, B and C). Therefore, these results revealed the effectiveness of lidocaine as it reached steady state in the second application of ATP (5 minutes), suggesting that lidocaine-mediated inhibition of the P2X7 receptor is use-dependent. More potent inhibition might be observed in the second application compared with the first because lidocaine would be able to access its site of

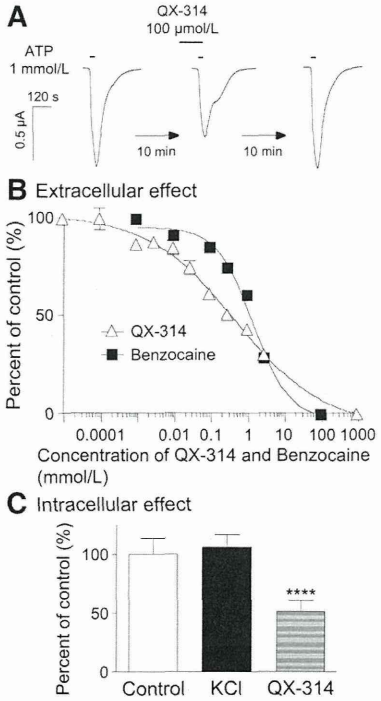

Figure 5. Effects of *N*-(2,6-dimethylphenylcarbamoylmethyl) triethylammonium bromide (QX-314) and benzocaine on adenosine triphosphate (ATP)-induced currents in oocytes expressing P2X7 receptor. A, Representative traces from oocytes expressing P2X7 receptors in both the absence and presence of extracellular 100 μmol/L QX-314. ATP was applied for 20 seconds with or without pretreatment for 2 minutes with 100 μmol/L QX-314. The currents of QX-314-treated oocytes were recorded 10 minutes after recording the control currents, and the washout currents were obtained 10 minutes after QX-314 treatment. B, Concentration–response curves for extracellular QX-314 and benzocaine-mediated inhibition on ATP-induced currents in oocytes expressing P2X7 receptors. The peak current amplitude in the presence of local anesthetics was normalized to that of the control, and the effects are expressed as percentages of the control. QX-314 and benzocaine reduced ATP-induced currents in a concentration-dependent manner with the half maximal inhibitory concentration (IC_{50}) values and slope variables of 500 ± 75 μmol/L and 0.36 ± 0.03, and 1.6 ± 0.04 mmol/L and 0.88 ± 0.07, respectively. C, Effects of intracellular QX-314 on ATP-induced currents in oocytes expressing P2X7 receptor. ATP-induced currents were recorded 10 minutes after intracellular injection of 5 mmol/L QX-314 diluted by 150 mmol/L potassium chloride (KCl), resulting in intracellular concentration of 500 μmol/L and intracellular injection of 150 mmol/L KCl as control cells. Intracellular injection of QX-314 significantly suppressed ATP-induced currents to 51 ± 9% of control although that of 150 mmol/L KCl did not reduce those currents. Data are presented as means ± SEM (n = 6). Hill coefficient and IC_{50} values were calculated using GraphPad Prism. ****P < 0.0001 compared with the control (one-way analysis of variance followed by Dunnett post hoc test).

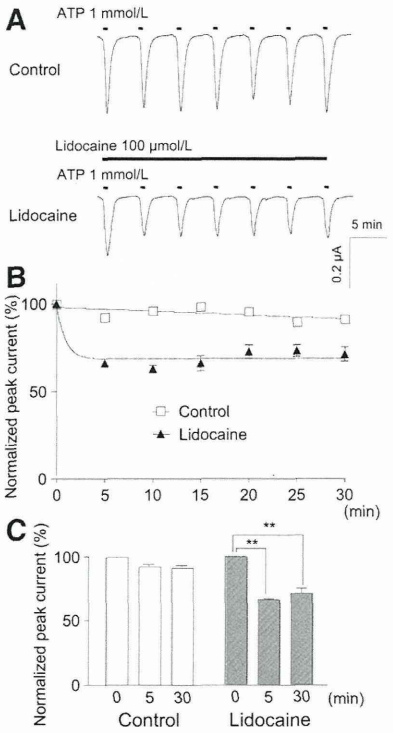

Figure 6. Analyses of use dependency of lidocaine block on P2X7 receptor. Repetitive application of 1 mmol/L adenosine triphosphate (ATP; 20 seconds) at 5-minute intervals was done in the absence or continuous presence of 100 μmol/L lidocaine for 30 minutes. A, Representative traces induced by repetitive ATP application for 30 minutes from oocytes expressing P2X7 receptors in the absence or continuous presence of 100 μmol/L lidocaine. All typical traces were obtained from the same oocyte. B, Peak currents were normalized to the first pulse and plotted against the pulse number. C, Comparison of the normalized currents between the first (0 minute), second (5 minutes), and seventh (30 minutes) applications. In the continuous presence of lidocaine, the responses to the second application of ATP (5 minutes) were significantly reduced to 66% ± 3% of currents induced by the first application of ATP (0 minute). However, inhibitory effect at seventh application (30 minutes) was statistically the same as that at second application (5 minutes). Data are expressed as means ± SEM (n = 6). **P < 0.01 compared with the control (one-way analysis of variance followed by Tukey post hoc test).

action sufficiently during a 5-minute treatment, whereas the first application in which lidocaine and ATP were simultaneously applied (no lidocaine pretreatment) would not be sufficient for lidocaine to access its site of action.

Effects of Selective P2X7 Receptor Antagonists on the Inhibitory Actions of Lidocaine

We next investigated the action of lidocaine in the absence and presence of selective antagonists of the P2X7 receptor, BBG, or AZ11645373 to determine whether these compounds modulate the inhibitory actions of lidocaine on the P2X7 receptor. Oocytes were pretreated with 1 μmol/L BBG or 300 nmol/L AZ11645373 2 minutes before coapplication of 10 μmol/L to 3 mmol/L lidocaine for 2 minutes (Fig. 7, A and B). Figure 7, C and D, shows normalized inhibition curves for lidocaine in the absence and presence of preapplied and coapplied BBG or AZ11645373. The IC_{50} values and slope variables of the lidocaine concentration–response curves with BBG or AZ11645373 were 315 ± 56 μmol/L and 0.92 ± 0.14, or 258 ± 52 μmol/L and 0.93 ± 0.18, respectively. This suggests that neither BBG nor AZ11645373 modulated the effects of lidocaine, which exhibited an IC_{50} value and slope variable of 282 ± 45 μmol/L and 0.72 ± 0.07, respectively (P = 0.658 and 0.237, or P = 0.736 and 0.309, respectively, for the IC_{50} values and the slope variables of the lidocaine concentration–response curves with BBG or AZ11645373, 99% CI, −132.7 to 198.7 and −0.161 to 0.561, or −134.6 to 182.6 and

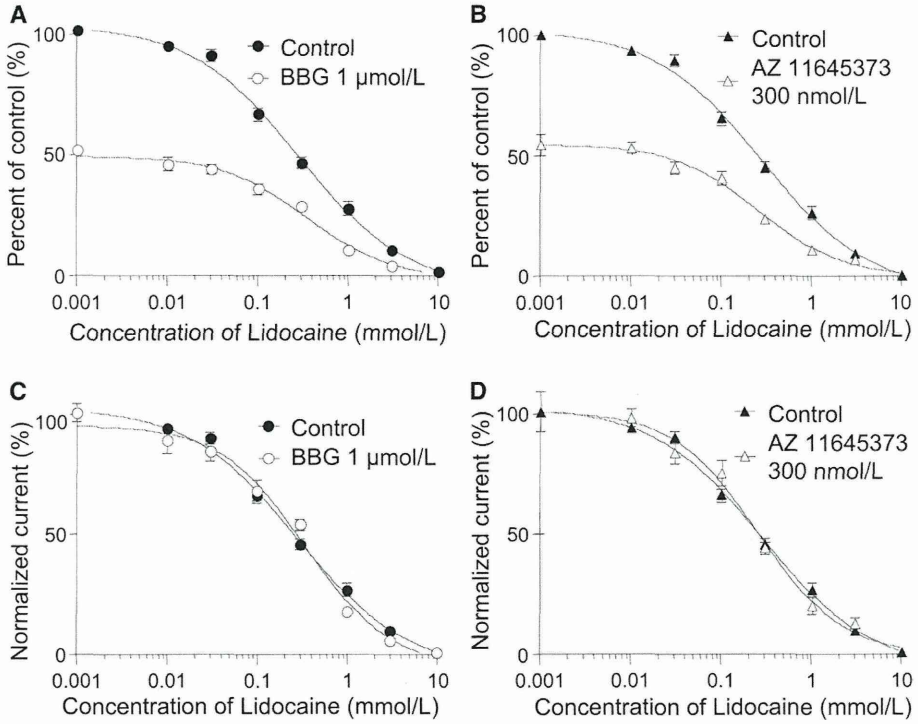

Figure 7. *Consentration-response curves for lidocaine inhibition in the absence or presence of pre-treatment for 4-min by 1 μmol/L BBG (A) or 300 nmol/L AZ11645373 (B). BBG or AZ11645373 were pre-applied for 2 min prior to co-application with lidocaine (10 μmol/L–3 mmol/L) for 2 min. Normalized inhibition curves for lidocaine in the absence and presence of BBG (C) or AZ11645373 (D) were obtained from (A) and (B). Both BBG and AZ11645373 did not affect inhibitory effect of lidocaine on P2X7 receptor; the IC50 values and slope variables were 282 ± 45 μmol/L and 0.72 ± 0.07, 315 ± 56 μmol/L and 0.92 ± 0.14, and 258 ± 52 μmol/L and 0.93 ± 0.18, in control, BBG, and AZ11645373 pre-treatment, respectively. Data are expressed as means ± SEM (n = 6). Hill coefficient, IC50 values were calculated using GraphPad Prism. ATP = adenosine triphosphate; BBG = Brilliant Blue G; IC50 = half maximal inhibitory concentration.*

−0.235 to 0.655). Overall, these data suggest that lidocaine interacts with a different site on the P2X7 receptor from the sites of action of either BBG or AZ11645373, which are non-competitive antagonists of the P2X7 receptor.

DISCUSSION

In the present study, we demonstrated that lidocaine selectively inhibited ATP-induced inward currents of the P2X7 receptor in a concentration-dependent manner. To our knowledge, this study is the first direct evidence that lidocaine suppresses the P2X7 receptor. Substantial pain relief is achieved at plasma concentrations of 2 to 5 μg/mL (7–20 μmol/L) by continuous infusion of lidocaine in cancer patients with neuropathic pain.[33] In the present study, the IC_{50} value of lidocaine-mediated P2X7 inhibition was 282 ± 45 μmol/L. Lidocaine tended to suppress ATP-induced currents at concentrations ≥10 μmol/L, and these inhibitory effects were significant at concentrations ≥30 μmol/L ($P < 0.001$). Although it is not proven whether a small inhibitory effect (7% inhibition) of lidocaine at 10 μmol/L produces pain relief in systemic administration, lidocaine might suppress P2X7 function at least when it is administered locally such as epidural administration because P2X7 receptors are expressed on glial cells in spinal neurons.

Lidocaine had little effect on the P2X3 and P2X4 receptors, but selectively suppressed the function of P2X7 receptors. The P2X7 receptor is structurally distinct from other P2X receptors; it also has different gating properties although these are only poorly understood.[34] The P2X7 receptor is permeable not only to small cations (sodium, potassium, and calcium) as similar to other subunits but also to larger cations such as *N*-methyl-D-glucamine and nanometer-sized dyes,[35] probably through the progressive dilation of the pore or the opening of a distinct accessory channel.[36] Therefore, it is of great interest to explore how lidocaine inhibits the function of the P2X7 receptor alone. Lidocaine would not affect three ATP-binding sites that are shown to exist in the extracellular region of P2X receptors[37] because lidocaine-mediated inhibition was found to be noncompetitive in this study. Moreover, lidocaine-mediated inhibition of the P2X7 receptor was use-dependent. Taken together, these findings suggest that lidocaine exerts its effects by affecting the site in the ion channel pore. By contrast, the inhibitory effects of QX-314 and benzocaine suggest that both charged and uncharged local anesthetics can also suppress P2X7 function. Moreover, intracellular injection of the charged local anesthetic QX-314 also inhibited P2X7 function. These results suggest that lidocaine acts on both intracellular and extracellular sites of the P2X7 receptor and that both charged and uncharged lidocaine could modulate this receptor.

We demonstrated that other local anesthetics including mepivacaine, ropivacaine, and bupivacaine have only limited effects on P2X7 receptor function. All these three

compounds, but not lidocaine, contain a piperidine ring (Fig. 8), to which is attached a carbon chain of different lengths; one carbon in mepivacaine, three in ropivacaine, and four in bupivacaine. Therefore, it is possible that the piperidine ring is an obstacle to the action of local anesthetics because the inhibitory potency of mepivacaine was one-twentieth of that of lidocaine. Moreover, longer carbon chains connected to the piperidine ring may further hinder potential effects because both ropivacaine and bupivacaine had little effect on the P2X7 receptor. Therefore, it is possible that lidocaine suppresses P2X7 receptor function by acting on a binding site in the ion channel. Recent X-ray crystal structural analyses of P2X4 receptor in zebrafish revealed that P2X receptors exhibit homotrimeric architecture and that each subunit consists of a large hydrophilic extracellular domain and a transmembrane domain composed of two α-helices, which resemble the shape of a dolphin.[38,39] These analyses also revealed that binding of ATP to the ATP-binding pocket within an intersubunit cleft rotates each subunit, resulting in promotion of the ion channel pore opening. P2X3, P2X4, and P2X7 are 40% to 50% identical in amino acid sequence, and each subunit of the P2X7 receptor has a longer amino acid sequence (595) than P2X3 (397) and P2X4 (388) because only P2X7 has a long intracellular C-terminus. Therefore, lidocaine might bind to the binding pocket for local anesthetics that exists mainly in the P2X7 receptor because of the differences of amino acid sequence to prevent the subunits from rotating that leads to channel opening.

Many P2X7 receptor antagonists have been reported in addition to antagonists of other P2X receptor subunits although they are not used clinically.[34] Some antagonists, including pyridoxal phosphate-6-azophenyl-2′,4′-disulfonic acid and periodate-oxidized ATP, were demonstrated to interact at the ATP-binding sites, showing that they were competitive antagonists.[40] By contrast, many of them inhibit P2X7-mediated responses by acting in a noncompetitive manner. We examined whether BBG and AZ11645373 interact with the inhibitory action of lidocaine on P2X7 receptors because these two compounds are selective P2X7 inhibitors and act in a similar noncompetitive manner to lidocaine. BBG was shown to produce a noncompetitive inhibition of rat P2X7 receptors more potently than human P2X7 receptors; IC_{50} values were 10 and 200 nmol/L, respectively,[41] whereas

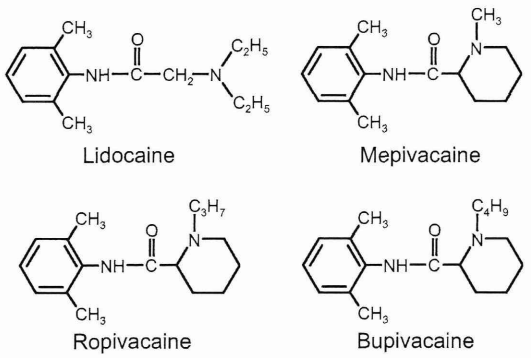

Figure 8. Structures of lidocaine, mepivacaine, ropivacaine, and bupivacaine.

it was reported that AZ11645373 is a highly selective and potent antagonist at human, but not at rat, P2X7 receptors.[42] Our data suggested that lidocaine acts on a different site of the P2X7 receptor than both BBG and AZ11645373.

The systemic administration of lidocaine has been considered to reduce neuropathic pain via suppression of ectopic activity by inhibiting abnormally expressed voltage-gated sodium channels.[5] One study demonstrated that the incidence of C-fibers with ongoing activity was significantly reduced by systemic administration of lidocaine resulting in low plasma concentrations in a chronic inflammatory model.[43] However, it was also shown that this effect was only partially correlated with chronic pain relief compared with the complete inhibition of spontaneous discharge in C-fibers, suggesting that there may be mechanisms other than blocking sodium channel activity. Moreover, many reports demonstrate that lidocaine also affects other pain signaling pathways.[6] It has been demonstrated that intravenous lidocaine infusion increased acetylcholine concentrations in cerebrospinal fluid, which exacerbated inhibitory descending pain pathways resulting in analgesia.[44] Lidocaine has also been shown to produce central inhibitory effects via spinal strychnine-sensitive glycine receptors[45] and to stimulate the release of endogenous opioids to promote its analgesic effect.[46] Moreover, lidocaine has been reported to reduce the postsynaptic depolarization mediated by *N*-methyl-D-aspartate and neurokinin receptors,[47] and a study in a recombinant model demonstrated that local anesthetics, including lidocaine, directly inhibited the activation of human *N*-methyl-D-aspartate receptors in a concentration-dependent manner.[48]

The P2X7 receptor is expressed predominantly on immune cells and has been shown to play an important role in the inflammatory response by demonstrating that activation of the P2X7 receptor leads to maturation and release of interleukin (IL)-1β and initiation of a cytokine cascade.[49,50] Several reports also suggest a role for the P2X7 receptor in pain modulation because systemic administration of selective antagonists of P2X7 receptors produced antinociceptive effects,[51] and hypersensitivity was not observed in P2X7-knockout mice[52] in neuropathic and inflammatory pain models. In addition, some reports suggest that lidocaine exerts anti-inflammatory effects by suppressing cytokine-induced injury[53] or attenuating the production of proinflammatory cytokines including tumor necrosis factor-α, IL-1β, and IL-6 induced by extracellular ATP in microglia.[54] Taken together, these data indicate that P2X7 receptor antagonists might be beneficial for the treatment of neuropathic and inflammatory pain. Therefore, suppression of the P2X7 receptor might be a mechanism underlying the anti-inflammatory effects and chronic pain relief affected by lidocaine. Although our present results suggest that the P2X3 and P2X4 receptors are not involved in the mechanism of lidocaine-induced pain relief, further experiments are needed to investigate the effects on other subunits including P2X2/3 or P2Y12, which are also related to chronic pain. Although ropivacaine and bupivacaine can relieve neuropathic pain effectively by epidural administration, P2X7 signaling would not be involved in their mechanism underlying pain relief.

In conclusion, lidocaine selectively inhibited ATP-induced currents of P2X7 receptors expressed in *Xenopus*

oocytes at clinically relevant concentrations when it was administered locally at least. The effect of lidocaine on P2X7 receptors was likely a result of noncompetitive inhibition at both extracellular and intracellular sites in the ion channel pore. To our knowledge, these results are the first evidence showing novel lidocaine-mediated effects on P2X receptors in a recombinant experimental system and might become the key to elucidate the mechanisms of pain relief by lidocaine. However, further studies are needed to clarify the relevance of P2X7 receptor inhibition of the analgesic effects of lidocaine.

DISCLOSURES

Name: Dan Okura, MD.
Contribution: This author conducted data collection, data analysis, and manuscript preparation.
Attestation: Dan Okura approved the final manuscript, and attests to the integrity of the original data and the analysis reported in this manuscript.
Name: Takafumi Horishita, MD, PhD.
Contribution: This author helped study design, data collection, data analysis, and manuscript preparation.
Attestation: Takafumi Horishita approved the final manuscript, attests to the integrity of the original data and the analysis reported in this manuscript and also is the archival author.
Name: Susumu Ueno, MD, PhD.
Contribution: This author helped design the study, and prepare the manuscript.
Attestation: Susumu Ueno approved the final manuscript.
Name: Nobuyuki Yanagihara, PhD.
Contribution: This author helped prepared the manuscript.
Attestation: Nobuyuki Yanagihara approved the final manuscript.
Name: Yuka Sudo, PhD.
Contribution: This author helped prepare the manuscript.
Attestation: Yuka Sudo approved the final manuscript.
Name: Yasuhito Uezono, MD, PhD.
Contribution: This author helped prepare the manuscript.
Attestation: Yasuhito Uezono approved the final manuscript.
Name: Tomoko Minami, MD.
Contribution: This author helped prepare the manuscript.
Attestation: Tomoko Minami approved the final manuscript.
Name: Takashi Kawasaki, MD, PhD.
Contribution: This author helped prepare the manuscript.
Attestation: Takashi Kawasaki approved the final manuscript.
Name: Takeyoshi Sata, MD, PhD.
Contribution: This author helped conduct the study and prepare the manuscript.
Attestation: Takeyoshi Sata approved the final manuscript.
This manuscript was handled by: Markus W. Hollmann, MD, PhD, DEAA.

REFERENCES

1. Mao J, Chen LL. Systemic lidocaine for neuropathic pain relief. Pain 2000;87:7–17
2. Buchanan DD, J MacIvor F. A role for intravenous lidocaine in severe cancer-related neuropathic pain at the end-of-life. Support Care Cancer 2010;18:899–901
3. Lai J, Hunter JC, Porreca F. The role of voltage-gated sodium channels in neuropathic pain. Curr Opin Neurobiol 2003;13: 291–7
4. Baron R, Binder A, Wasner G. Neuropathic pain: diagnosis, pathophysiological mechanisms, and treatment. Lancet Neurol 2010;9:807–19
5. Amir R, Argoff CE, Bennett GJ, Cummins TR, Durieux ME, Gerner P, Gold MS, Porreca F, Strichartz GR. The role of sodium channels in chronic inflammatory and neuropathic pain. J Pain 2006;7:S1–29
6. Groudine SB, Fisher HA, Kaufman RP Jr, Patel MK, Wilkins LJ, Mehta SA, Lumb PD. Intravenous lidocaine speeds the return of bowel function, decreases postoperative pain, and shortens hospital stay in patients undergoing radical retropubic prostatectomy. Anesth Analg 1998;86:235–9
7. Cooke ED, Bowcock SA, Lloyd MJ, Pilcher MF. Intravenous lignocaine in prevention of deep venous thrombosis after elective hip surgery. Lancet 1977;2:797–9
8. Hollmann MW, Durieux ME. Local anesthetics and the inflammatory response: a new therapeutic indication? Anesthesiology 2000;93:858–75
9. Jänig W. What is the mechanism underlying treatment of pain by systemic application of lidocaine? Pain 2008;137:5–6
10. Hollmann MW, McIntire WE, Garrison JC, Durieux ME. Inhibition of mammalian Gq protein function by local anesthetics. Anesthesiology 2002;97:1451–7
11. Bräu ME, Nau C, Hempelmann G, Vogel W. Local anesthetics potently block a potential insensitive potassium channel in myelinated nerve. J Gen Physiol 1995;105:485–505
12. Xiong Z, Strichartz GR. Inhibition by local anesthetics of Ca^{2+} channels in rat anterior pituitary cells. Eur J Pharmacol 1998;363:81–90
13. North RA. Molecular physiology of P2X receptors. Physiol Rev 2002;82:1013–67
14. Lang PM, Sippel W, Schmidbauer S, Irnich D, Grafe P. Functional evidence for P2X receptors in isolated human vagus nerve. Anesthesiology 2003;99:232–5
15. Burnstock G, Knight GE. Cellular distribution and functions of P2 receptor subtypes in different systems. Int Rev Cytol 2004;240:31–304
16. Khakh BS, North RA. P2X receptors as cell-surface ATP sensors in health and disease. Nature 2006;442:527–32
17. Burnstock G. Pathophysiology and therapeutic potential of purinergic signaling. Pharmacol Rev 2006;58:58–86
18. Eltzschig HK, Sitkovsky MV, Robson SC. Purinergic signaling during inflammation. N Engl J Med 2012;367:2322–33
19. Eltzschig HK. Targeting purinergic signaling for perioperative organ protection. Anesthesiology 2013;118:1001–4
20. Gum RJ, Wakefield B, Jarvis MF. P2X receptor antagonists for pain management: examination of binding and physicochemical properties. Purinergic Signal 2012;8:41–56
21. Honore P, Kage K, Mikusa J, Watt AT, Johnston JF, Wyatt JR, Faltynek CR, Jarvis MF, Lynch K. Analgesic profile of intrathecal P2X(3) antisense oligonucleotide treatment in chronic inflammatory and neuropathic pain states in rats. Pain 2002;99:11–9
22. Tsuda M, Shigemoto-Mogami Y, Koizumi S, Mizokoshi A, Kohsaka S, Salter MW, Inoue K. P2X4 receptors induced in spinal microglia gate tactile allodynia after nerve injury. Nature 2003;424:778–83
23. Chessell IP, Hatcher JP, Bountra C, Michel AD, Hughes JP, Green P, Egerton J, Murfin M, Richardson J, Peck WL, Grahames CB, Casula MA, Yiangou Y, Birch R, Anand P, Buell GN. Disruption of the P2X7 purinoceptor gene abolishes chronic inflammatory and neuropathic pain. Pain 2005;114:386–96
24. Andoh T, Furuya R, Oka K, Hattori S, Watanabe I, Kamiya Y, Okumura F. Differential effects of thiopental on neuronal nicotinic acetylcholine receptors and P2X purinergic receptors in PC12 cells. Anesthesiology 1997;87:1199–209
25. Furuya R, Oka K, Watanabe I, Kamiya Y, Itoh H, Andoh T. The effects of ketamine and propofol on neuronal nicotinic acetylcholine receptors and P2x purinoceptors in PC12 cells. Anesth Analg 1999;88:174–80
26. Nakanishi M, Mori T, Nishikawa K, Sawada M, Kuno M, Asada A. The effects of general anesthetics on P2X7 and P2Y receptors in a rat microglial cell line. Anesth Analg 2007;104:1136–44
27. Xiong K, Hu XQ, Stewart RR, Weight FF, Li C. The mechanism by which ethanol inhibits rat P2X4 receptors is altered by mutation of histidine 241. Br J Pharmacol 2005;145:576–86
28. Nagata K, Imai T, Yamashita T, Tsuda M, Tozaki-Saitoh H, Inoue K. Antidepressants inhibit P2X4 receptor function: a

possible involvement in neuropathic pain relief. Mol Pain 2009;5:20
29. Horishita T, Eger EI II, Harris RA. The effects of volatile aromatic anesthetics on voltage-gated Na^+ channels expressed in *Xenopus* oocytes. Anesth Analg 2008;107:1579–86
30. Okura D, Horishita T, Ueno S, Yanagihara N, Sudo Y, Uezono Y, Sata T. The endocannabinoid anandamide inhibits voltage-gated sodium channels Nav1.2, Nav1.6, Nav1.7, and Nav1.8 in *Xenopus* oocytes. Anesth Analg 2014;118:554–62
31. Khakh BS, Bao XR, Labarca C, Lester HA. Neuronal P2X transmitter-gated cation channels change their ion selectivity in seconds. Nat Neurosci 1999;2:322–30
32. Roberts JA, Digby HR, Kara M, El Ajouz S, Sutcliffe MJ, Evans RJ. Cysteine substitution mutagenesis and the effects of methanethiosulfonate reagents at P2X2 and P2X4 receptors support a core common mode of ATP action at P2X receptors. J Biol Chem 2008;283:20126–36
33. Devulder JE, Ghys L, Dhondt W, Rolly G. Neuropathic pain in a cancer patient responding to subcutaneously administered lignocaine. Clin J Pain 1993;9:220–3
34. Coddou C, Yan Z, Obsil T, Huidobro-Toro JP, Stojilkovic SS. Activation and regulation of purinergic P2X receptor channels. Pharmacol Rev 2011;63:641–83
35. Browne LE, Compan V, Bragg L, North RA. P2X7 receptor channels allow direct permeation of nanometer-sized dyes. J Neurosci 2013;33:3557–66
36. Becker D, Woltersdorf R, Boldt W, Schmitz S, Braam U, Schmalzing G, Markwardt F. The P2X7 carboxyl tail is a regulatory module of P2X7 receptor channel activity. J Biol Chem 2008;283:25725–34
37. Browne LE, Jiang LH, North RA. New structure enlivens interest in P2X receptors. Trends Pharmacol Sci 2010;31:229–37
38. Kawate T, Michel JC, Birdsong WT, Gouaux E. Crystal structure of the ATP-gated P2X(4) ion channel in the closed state. Nature 2009;460:592–8
39. Hattori M, Gouaux E. Molecular mechanism of ATP binding and ion channel activation in P2X receptors. Nature 2012;485:207–12
40. Michel AD, Xing M, Thompson KM, Jones CA, Humphrey PP. Decavanadate, a P2X receptor antagonist, and its use to study ligand interactions with P2X7 receptors. Eur J Pharmacol 2006;534:19–29
41. Jiang LH, Mackenzie AB, North RA, Surprenant A. Brilliant blue G selectively blocks ATP-gated rat P2X(7) receptors. Mol Pharmacol 2000;58:82–8
42. Stokes L, Jiang LH, Alcaraz L, Bent J, Bowers K, Fagura M, Furber M, Mortimore M, Lawson M, Theaker J, Laurent C, Braddock M, Surprenant A. Characterization of a selective and potent antagonist of human P2X(7) receptors, AZ11645373. Br J Pharmacol 2006;149:880–7
43. Xiao WH, Bennett GJ. C-fiber spontaneous discharge evoked by chronic inflammation is suppressed by a long-term infusion of lidocaine yielding nanogram per milliliter plasma levels. Pain 2008;137:218–28
44. Abelson KS, Höglund AU. Intravenously administered lidocaine in therapeutic doses increases the intraspinal release of acetylcholine in rats. Neurosci Lett 2002;317:93–6
45. Biella G, Sotgiu ML. Central effects of systemic lidocaine mediated by glycine spinal receptors: an iontophoretic study in the rat spinal cord. Brain Res 1993;603:201–6
46. Cohen SP, Mao J. Is the analgesic effect of systemic lidocaine mediated through opioid receptors? Acta Anaesthesiol Scand 2003;47:910–1
47. Nagy I, Woolf CJ. Lignocaine selectively reduces C fibre-evoked neuronal activity in rat spinal cord in vitro by decreasing *N*-methyl-D-aspartate and neurokinin receptor-mediated postsynaptic depolarizations; implications for the development of novel centrally acting analgesics. Pain 1996;64:59–70
48. Hahnenkamp K, Durieux ME, Hahnenkamp A, Schauerte SK, Hoenemann CW, Vegh V, Theilmeier G, Hollmann MW. Local anaesthetics inhibit signalling of human NMDA receptors recombinantly expressed in *Xenopus laevis* oocytes: role of protein kinase C. Br J Anaesth 2006;96:77–87
49. Solle M, Labasi J, Perregaux DG, Stam E, Petrushova N, Koller BH, Griffiths RJ, Gabel CA. Altered cytokine production in mice lacking P2X(7) receptors. J Biol Chem 2001;276:125–32
50. Ferrari D, Pizzirani C, Adinolfi E, Lemoli RM, Curti A, Idzko M, Panther E, Di Virgilio F. The P2X7 receptor: a key player in IL-1 processing and release. J Immunol 2006;176:3877–83
51. Donnelly-Roberts DL, Jarvis MF. Discovery of P2X7 receptor-selective antagonists offers new insights into P2X7 receptor function and indicates a role in chronic pain states. Br J Pharmacol 2007;151:571–9
52. Clark AK, Staniland AA, Marchand F, Kaan TK, McMahon SB, Malcangio M. P2X7-dependent release of interleukin-1beta and nociception in the spinal cord following lipopolysaccharide. J Neurosci 2010;30:573–82
53. de Klaver MJ, Buckingham MG, Rich GF. Lidocaine attenuates cytokine-induced cell injury in endothelial and vascular smooth muscle cells. Anesth Analg 2003;97:465–70
54. Su D, Gu Y, Wang Z, Wang X. Lidocaine attenuates proinflammatory cytokine production induced by extracellular adenosine triphosphate in cultured rat microglia. Anesth Analg 2010;111:768–74

A cross-fostering analysis of bromine ion concentration in rats that inhaled 1-bromopropane vapor

Toru ISHIDAO[1], Yukiko FUETA[1], Susumu UENO[2], Yasuhiro YOSHIDA[3], and Hajime HORI[1]

[1] Department of Environmental Management, School of Health Sciences, University of Occupational and Environmental Health, Japan.

[2] Department of Occupational Toxicology, Institute of Industrial Ecological Sciences, University of Occupational and Environmental Health, Japan.

[3] Department of Immunology and Parasitology, School of Medicine, University of Occupational and Environmental Health, Japan.

Correspondence to: Toru Ishidao, Department of Environmental Management, School of Health Sciences, University of Occupational and Environmental Health, Japan. Iseigaoka 1-1, Yahatanishi-ku, Kitakyushu 807-8555, Japan

(*e-mail: ishidao@health.uoeh-u.ac.jp*)

Running title: **A cross-fostering analysis of bromine ion concentration**

The number of words in the abstract: **238**; text: **2087**, and the number of tables: **2**; figures: **3**

Field: ***Toxicology***

Abstract: Objective: Inhaled 1-bromopropane decomposes easily and releases bromine ion. However, the kinetics and transfer of bromine ion into the next generation have not been clarified. In this work, the kinetics of bromine ion transfer to the next generation was investigated by using cross-fostering analysis and a one-compartment model. **Methods:** Pregnant Wistar rats were exposed to 700 ppm of 1-bromopropane vapor for 6 h per day during gestation days (GDs) 1–20. After birth, cross-fostering was performed between mother exposure groups and mother control groups, and the pups were subdivided into the following four groups: exposure group, postnatal exposure group, gestation exposure group, and control group. Bromine ion concentrations in the brain were measured temporally. **Results:** Bromine ion concentrations in mother rats were lower than those in virgin rats, and the concentrations in fetuses were higher than those in mothers on GD20. In the postnatal period, the concentrations in the gestation exposure group decreased with time, and the biological half-life was 3.1 days. Conversely, bromine ion concentration in the postnatal exposure group increased until postnatal day 4 and then decreased. This tendency was also observed in the exposure group. A one-compartment model was applied to analyze the behavior of bromine ion concentration in the brain. By taking into account the increase of body weight and change in the bromine ion uptake rate in pups, the bromine ion concentrations in the brains of the rats could be estimated with acceptable precision.

Key words: 1-Bromopropane inhalation, Cross-fostering, Bromine ion concentration, One-compartment model, Animal experiment

1-Bromopropane (1-BP, CAS no. 106-94-5) is widely used as a substitute for chlorofluorocarbons, which destroy the ozone layer. The toxicity of 1-BP has been